

How many samples are needed to leverage smoothness?

Vivien Cabannes
Meta AI

Stefano Vigogna
Tor Vergata

May 26, 2023

Abstract

A core principle in statistical learning is that smoothness of target functions allows to break the curse of dimensionality. However, learning a smooth function through Taylor expansions requires enough samples close to one another to get meaningful estimate of high-order derivatives, which seems hard in machine learning problems where the ratio between number of data and input dimension is relatively small. Should we really hope to break the curse of dimensionality based on Taylor expansion estimation? What happens if Taylor expansions are replaced by Fourier or wavelet expansions? By deriving a new lower bound on the generalization error, this paper investigates the role of constants and transitory regimes which are usually not depicted beyond classical learning theory statements while that play a dominant role in practice.

1 Introduction

The current practice of machine learning consists in feeding a machine with many samples for it to infer a useful rule. In supervised learning, the samples are input/output (I/O) pairs, and the rule is a relationship to predict outputs from inputs. Once learned, the I/O mapping can be deployed in the wild to infer useful information from new inputs. Because it was not engineered by hands, one can question the mapping correctness. How to make sure that this rule will not lead to unwanted behaviors? The classical answer to this question lies in statistics. Assuming that the training samples are independent and identically distributed according to the future use cases, it is possible to derive theorems akin to the central limit theorem.

While many statistical learning principles could offer practical insights, theoretical results often appear somewhat obscure, and forming intuition about them is often challenging, which limits their impact. In this paper, we focus on one simple principle: “smoothness allows to break the curse of dimensionality”. The curse of dimensionality is a generic term referring to a set of high-dimensional phenomena with significant practical consequences. In supervised learning, it manifests as follows: without a good prior on the I/O mapping to be learned, one can only get good estimates of the mapping close to the observed examples; as a consequence, to obtain a good global estimate, one needs to collect enough data points to finely cover the input space, which implies that the number of data points should scale exponentially with the dimension of the input space. Yet, when provided with the information that the mapping has some structure, one might need significantly less examples to learn from. This is notably the case when the mapping is assumed to be smooth. The goal of this paper is to better understand how and when we can expect to get much better convergence guarantees when the target function is known to be smooth.

Related work. Nonparametric local estimators were introduced as soon as the field of learning began to form in the 50’s [10], and their consistency were studied extensively in the second half of the twentieth century (see Stone [27], Devroye et al. [8] and references therein). Introduced for scatter plots [7], local polynomials were the first estimators to leverage smoothness to improve regression [11]. They were later replaced by kernel methods, which are a powerful way to adapt to smoothness without much fine-tuning, and were widely regarded as state-of-the-art before the deep learning era [23]. Convergence results for kernel methods can be understood through the size of their associated functional spaces [12, 30], how those sizes relate to generalization guarantees [29], and how those

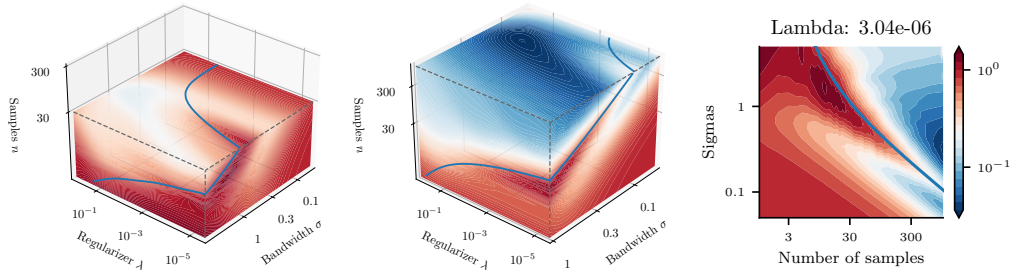


Figure 1: Log-log-log-log plots of excess risk (in color) with respect to the number of samples (z -axis), the regularizer λ (x -axis) and the bandwidth σ (y -axis) when $f^*(x) = \text{sign}(\langle x, e_1 \rangle)$ and $\rho_{\mathcal{X}}$ is uniform on $[-1, 1]^2$. Asymptotically, there exists some (λ_n, σ_n) to ensure that the excess risk decreases in $O(n^{-\gamma})$ for a γ predicted by theory. However, for finite values of n , the excess risk can present different power law decays. Those transitory regimes, where the behavior of the excess risk can be quite different than its asymptotic “stationary” behavior, are usually not well described by theory, while they might be the dominating regimes in applied machine learning when the number of samples is relatively small compared to the input dimension. The dark blue line on each plot indicates the transition between low- and high-sample regime: it corresponds to the graph $\{(\sigma, \lambda, n) \mid n = \mathcal{N}_1(\sigma, \lambda)\}$. The figure illustrates a double descent phenomenon where excess risk peaks are reached when $n = \mathcal{N}_1$ before a second descent takes place. Those peaks can be avoided in practice by computing the effective dimension \mathcal{N} and tuning hyperparameters to ensure it to be smaller than n .

spaces adhere to L^2 [20, 24]. For least-squares regression, relations between the size of those spaces and generalization guarantees are usually derived through operator concentration [25, 6]. More recently, transitory regime behaviors were described in Mei et al. [15], Mei and Montanari [14], and high-dimensional phenomena that lift the need to have more data than dimensions were studied in [21, 13], with Bach [3] relating the latter analyses with the former ones.

Contributions. This work focuses on the role of smoothness in breaking the curse of dimensionality for typical supervised learning problems. At a high-level, our main contribution is to showcase the importance of transitory regimes where one does not have enough samples to leverage high-order smoothness (see Figure 6 for an illustration of transitory regimes). This arguably explains the poor performance of kernel methods without strong kernel engineering in the deep learning area: they try to leverage smoothness, but usually do not access enough samples to meaningfully estimate high-order derivatives. More precisely, our contributions are four-folds:

- We prove a new upper and lower bound theorem on the generalization error for penalized empirical risk minimization that holds for any function, and allows us to get a fine-grained picture of some of the transitory regimes where learning takes place in practice.
- We explain how Taylor expansion estimation is cursed by dimensionality due to the highly increasing (w.r.t. d) number of polynomials of degree α in dimension d .
- We explain how kernel ridge regression is cursed by dimensionality due to the highly increasing number of regular functions (e.g. trigonometric polynomials below a cut-off frequency) in dimension d .
- We expand on transitory regimes that are described by usual convergence theorems when working on constants more precisely.

All results are illustrated by numerical experiments, some of them to be found in Appendix C.

2 Abstract theoretical results

This section reviews classical results in learning theory, introduces a theory-friendly setup to study convergence rates, and derives a new lower bound on convergence rates that will be useful to describe theoretical learning limits in the following sections.

Supervised learning is concerned with learning a function from an input space \mathcal{X} to an output space \mathcal{Y} from a dataset $\mathcal{D}_n = (X_i, Y_i)_{i \in [n]}$ of $n \in \mathbb{N}$ examples. A learning rule, or algorithm, is a

mapping $\mathcal{A} : \mathcal{D}_n \mapsto f_n$ that builds a function $f_n : \mathcal{X} \rightarrow \mathcal{Y}$ based on the dataset \mathcal{D}_n , with the goal of capturing the underlying I/O relation. To discuss generalization to unseen examples, it is standard to model both the already collected and the future examples as independent realizations of a random pair (X, Y) following an unknown distribution ρ on $\mathcal{X} \times \mathcal{Y}$. For simplicity, we will assume $\mathcal{Y} = \mathbb{R}$ and $\mathcal{X} = \mathbb{R}^d$, or $\mathcal{X} = \mathbb{T}^d$ being the torus. The quality of a mapping $f : \mathcal{X} \rightarrow \mathcal{Y}$ is measured through the excess risk

$$\mathcal{E}(f) = \mathcal{R}(f) - \mathcal{R}(f^*) = \|f - f^*\|_{L^2(\rho_X)}^2, \quad (1)$$

where ρ_X is the marginal distribution of ρ on \mathcal{X} and, assuming that $(Y | X = x)$ has a second order moment for every $x \in \mathcal{X}$,

$$f^*(x) = \mathbb{E}[Y | X = x], \quad \text{which minimizes} \quad \mathcal{R}(f) = \mathbb{E}[|f(X) - Y|^2]. \quad (2)$$

The risk $\mathcal{R}(f)$ represents the average error of guessing $f(X)$ in place of Y when the error is measured through the least-squares loss. From a statistical viewpoint, it is useful to model $f_n = \mathcal{A}(\mathcal{D}_n)$ as a random function (inheriting its randomness from the samples), so to study the expectation or the upper tail of the excess risk $\mathcal{E}(f_n)$. Provided that f^* is measurable, it is possible to find methods such that $\mathcal{E}(f_n)$ converges to zero in probability. Without additional assumptions on f^* , it is not possible to give any guarantee on the speed of this convergence [11, Theorem 3.1]. However, when f^* is assumed to be smooth, the picture improves consequently.

Theorem 1 (Breaking the curse of dimensionality [11, 4]). *When f^* is α -smooth for $\alpha > 0$ in the sense that it admits $\lfloor \alpha \rfloor$ derivatives that are regular, more precisely if $f^* \in C^\alpha$ (i.e. f is α -Hölder regular), or $f^* \in H^\alpha = W^{\alpha,2}$ (i.e. f is α -Sobolev regular), there exists a learning rule $f_n = \mathcal{A}(\mathcal{D}_n)$ that guarantees*

$$\mathbb{E}_{\mathcal{D}_n}[\mathcal{E}(f_n)] \leq cn^{-2\alpha/(2\alpha+d)}, \quad (3)$$

where c is a constant independent of n . Moreover, the bound (3) is minimax optimal, in the sense that for any rule $f_n = \mathcal{A}(\mathcal{D}_n)$ there exists a distribution ρ such that $f^* \in C^\alpha$, or $f^* \in H^\alpha$, and the upper bound (3) holds as a lower bound with a different constant c .

Why do constants matter? At first glance, when two algorithms \mathcal{A}_1 and \mathcal{A}_2 guarantee two different upper bounds $O(n^{-\gamma_1})$ and $O(n^{-\gamma_2})$ on the expected excess risk, \mathcal{A}_1 will be deemed superior to \mathcal{A}_2 if $\gamma_1 \geq \gamma_2$, since after a certain number of samples, we will have that $\mathbb{E}_{\mathcal{D}_n}[\mathcal{A}_1(\mathcal{D}_n)] \leq \mathbb{E}_{\mathcal{D}_n}[\mathcal{A}_2(\mathcal{D}_n)]$. However, the constants hidden in the front of the big O s might lead to a different picture when given a small number of samples: \mathcal{A}_1 might actually be a so-called “galactic algorithm”, similarly to Strassen’s algorithm for matrix multiplication, that might not be worth using without a indecently large number of samples. This paper will show how classical algorithms that reach the minimax optimal convergence rates (3) present constants that are exponential in the dimension. It will equally show how the classical convergence analysis can be retaken to prove other convergence rates, with worse exponents γ but better constants, allowing to get a better picture of convergence rates in practical machine learning setups.

2.1 Hilbertian setup

To provide a fine-grained analysis of the phenomena at stake, we will focus on linear classes of functions. More exactly, we shall consider a feature map $\varphi : \mathcal{X} \rightarrow \mathcal{H}$, with \mathcal{H} a Hilbert space and $\varphi \in L^2(\rho_X)$. The map φ linearly parameterizes the space of functions

$$\mathcal{F} = \{f_\theta : x \mapsto \langle \varphi(x), \theta \rangle_{\mathcal{H}} \mid \theta \in \mathcal{H}\} \subset L^2(\rho_X). \quad (4)$$

For example, \mathcal{H} could be \mathbb{R}^k , φ seen as defining k features $\varphi_i(x)$ on inputs $x \in \mathcal{X}$. This model can be used to estimate f^* through the empirical risk minimizer

$$f_n \in \arg \min_{f \in \mathcal{F}} \sum_{i \in [n]} |f(X_i) - Y_i|^2. \quad (5)$$

In order to ensure that \mathcal{F} can learn any function f^* , the features can be enriched by concatenating a countably infinite number of features together. In this setting, it is more convenient to describe the geometry induced by \mathcal{F} through the (reproducing) kernel $k : \mathcal{X} \times \mathcal{X} \rightarrow \mathbb{R}$ defined as $k(x, x') = \langle \varphi(x), \varphi(x') \rangle$. Despite their apparent simplicity, reproducing kernels k describe rich spaces of functions \mathcal{F} known as reproducing kernel Hilbert space (RKHS), i.e. any Hilbert space of functions with continuous pointwise evaluations [2]. Classical examples are provided by subspaces of analytical functions C^ω through the Gaussian kernels $k(x, x') = \exp(-\|x - x'\|^2 / \sigma^2)$, and by the Sobolev space $H^{(d+1)/2}$ through the exponential kernel $k(x, x') = \exp(-\|x - x'\| / \sigma)$. When \mathcal{F} can fit too many functions, the estimate (5) needs to be refined to avoid overfitting. This paper will focus on Tikhonov (also known as ridge) regularization

$$f_{n,\lambda} \in \arg \min_{f \in \mathcal{F}} \sum_{i \in [n]} |f(X_i) - Y_i|^2 + n\lambda \|f\|_{\mathcal{F}}^2, \quad \lambda > 0, \quad (6)$$

where the norm is defined from (4) as $\|f\|_{\mathcal{F}} = \inf \{\|\theta\| \mid f = f_\theta\}$, but can also be expressed with the sole usage of k through the integral operator $K : L^2(\rho_{\mathcal{X}}) \rightarrow L^2(\rho_{\mathcal{X}})$,

$$Kf(x) = \int_{\mathcal{X}} k(x, x') f(x') \rho_{\mathcal{X}}(dx') = \mathbb{E}_X[k(x, X) f(X)], \quad (7)$$

as $\|f\|_{\mathcal{F}} = \|K^{-1/2}f\|_{L^2(\rho_{\mathcal{X}})}$, with the convention $K^{-1}(\ker K) = \{+\infty\}$.

Regularization is a change of kernel. In practice, positive kernels $k : \mathcal{X} \times \mathcal{X} \rightarrow \mathbb{R}$ are often defined through a base kernel together with hyperparameters. For example, kernels associated with local polynomials are parameterized by a partition on \mathcal{X} and a degree d . Similarly, many kernels present an explicit bandwidth $\sigma > 0$, e.g. translation-invariant kernels are defined as $k_\sigma(x, y) = q((x - y)/\sigma)$ for a function $q : \mathcal{X} \rightarrow \mathbb{R}$. The regularization parameter λ appearing in (6) can be incorporated as a specific hyperparameter of the kernel by setting $\lambda = 1$ in (6) and replacing k by $\lambda^{-1}k$. Geometrically, a change of λ leads to an isotropic rescaling of the ball $\|\cdot\|_{\mathcal{F}}^{-1}\{1\}$ inside $L^2(\rho_{\mathcal{X}})$, while a change of σ could favor certain directions (e.g. functions whose variations match the new bandwidth), or even remove some functions in \mathcal{F} (e.g. if the eigenvalues of K decrease exponentially fast).

2.2 Backbone analysis

The usual proof of Theorem 1 relies on theorems such as Theorem 2 below. Its formulation relates to the usual variance-bias trade-off in statistics, revisited as the estimation versus approximation error in statistical learning. A first term, the variance or the estimation error, depends on the variance of the data in ε^2/n and the capacity of the search space, captured by the effective dimension $\mathcal{N}_2(\lambda)$. A second term, the bias or the approximation error, captures the distance of the target function to the function class \mathcal{F} through a form of proximal projection $\mathcal{B}(\lambda)$. The two central terms are

$$\mathcal{N}_2(\lambda) = \text{Tr}(K^2(K + \lambda)^{-2}) \quad \text{and} \quad \mathcal{B}(\lambda) = \|K(K + \lambda)^{-1}f^* - f^*\|_{L^2(\rho_{\mathcal{X}})}^2. \quad (8)$$

The bias can be rewritten into a simpler source profile $\mathcal{S}(\lambda)$ as

$$\mathcal{B}(\lambda) = \lambda^2 \mathcal{S}(\lambda), \quad \mathcal{S}(\lambda) = \|(K + \lambda)^{-1}f^*\|_{L^2(\rho_{\mathcal{X}})}^2. \quad (9)$$

Theorem 2 (High-sample regime learning behavior). *Given n i.i.d. samples $\mathcal{D}_n = (X_i, Y_i)_{i \in [n]} \sim \rho^{\otimes n}$, when the noise in the labels $\varepsilon^2 = \text{ess sup var}(Y \mid X)$ does not depend on X (homoscedasticity), under two mild technical Assumptions 1 and 2, there exists a constant c such that, for any f^* in the closure of \mathcal{F} in $L^2(\rho_{\mathcal{X}})$, the estimate (6) verifies*

$$\left| \mathbb{E}_{\mathcal{D}_n} [\mathcal{E}(f_{\lambda,n})] - \frac{\varepsilon^2 \mathcal{N}_2(\lambda)}{n} - \lambda^2 \mathcal{S}(\lambda) \right| \leq c \mathcal{N}_1(\lambda) \left(a_n \cdot \frac{\varepsilon^2 \mathcal{N}_1(\lambda)}{n} + a_n^{1/2} \lambda^2 \mathcal{S}(\lambda) \right) \quad (10)$$

where $a_n = \mathcal{N}_\infty(\lambda)/n$, $\mathcal{N}_1(\lambda) = \text{Tr}(K(K + \lambda)^{-1})$, and $\mathcal{N}_\infty(\lambda) = \text{ess sup}_{x \sim \rho_{\mathcal{X}}} \text{Tr}(K_x(K + \lambda)^{-1})$ with K_x the rank-one operator on $L^2(\rho_{\mathcal{X}})$ that maps f to the constant function equal to $\mathbb{E}[f]k(x, x)$.

Theorem 2, proved in Appendix A.3, states that the generalization error $\mathbb{E}_{\mathcal{D}_n}[\mathcal{E}(f_{\lambda,n})]$ behaves as $A(n, \lambda) := \varepsilon^2 \mathcal{N}_2(\lambda)/n + \lambda^2 \mathcal{S}(\lambda)$ up to higher order terms specified in the right-hand side. We expect the right-hand side to be improvable with the removal of $\mathcal{N}_1(\lambda)$ in front of the rates (which is due to our usage of concentration inequalities on operators rather than on scalar values), the change of the second \mathcal{N}_1 into \mathcal{N}_2 , and the substitution of $a_n^{1/2}$ by a_n . This would show that $\mathbb{E}_{\mathcal{D}_n}[\mathcal{E}(f_{\lambda,n})]$ behaves as $A(n, \lambda)(1 + O(a_n))$. In the following, we will call very high-sample regimes situations where $a_n \leq 1$, and *high-sample regimes* situations where $\mathcal{N}_2(\lambda) \leq n$. Theorem 2 also holds for ridge-less regression (5) with $\lambda = 0$, $\mathcal{N}_1(\lambda) = \mathcal{N}_2(\lambda) = \dim \mathcal{F}$, $\mathcal{N}_\infty(\lambda) = \|K^{-1}\|^{-1} \|\varphi\|_\infty$, and $\lambda^2 \mathcal{S}(\lambda) = \|f^* - \pi_{\mathcal{F}} f^*\|^2$, where $\pi_{\mathcal{F}}$ is the $L^2(\rho_{\mathcal{X}})$ -orthogonal projection onto \mathcal{F} . In this setting, $\mathbb{E}_{\mathcal{D}_n}[\mathcal{E}(f_n)] = A(n, 0)(1 + O(n^{-1}))$, and the high-sample regime is characterized by $\dim \mathcal{F} \leq n$. Theorem 2 introduces subtle variations of \mathcal{N}_2 with \mathcal{N}_1 and \mathcal{N}_∞ , which can be thought as all behaving similarly with λ when ρ does not present heavy tails. Indeed, under the interpolation property $K^p(L^2(\rho_{\mathcal{X}})) \hookrightarrow L^\infty(\rho_{\mathcal{X}})$, i.e. $\|K^p f\|_\infty \leq \|f\|_{L^2(\rho_{\mathcal{X}})}$, which holds for classical Sobolev spaces $\mathcal{F} = H^\beta$ with $p = d/4\beta$, one can show that $\mathcal{N}_2(\lambda) \leq \mathcal{N}_1(\lambda) \leq \mathcal{N}_\infty(\lambda) = O(\lambda^{-2p})$. Regarding the second term $\lambda^2 \mathcal{S}(\lambda)$, it will decrease in $O(\lambda^{2q})$ under the source condition $f^* \in K^q(L^2(\rho_{\mathcal{X}}))$, which holds with $q = \alpha/2\beta$ when $f^* \in H^\alpha$ and $\mathcal{F} = H^\beta$. Details are provided in Appendix A.5.

Adaptive algorithms. This paper considers a similar meta-algorithm for all the discussed methods. It consists of defining an increasing family of function classes parameterized by some index $t \in \mathbb{R}$, formally $\mathcal{F} = \cup_{t>0} \mathcal{F}_t$, with $\mathcal{F}_t \subset \mathcal{F}_{t+dt}$ for any $t, dt > 0$. For example, \mathcal{F}_t could be defined from a fixed feature map φ as a ball of radius t with $\mathcal{F}_t = \{f \in \mathcal{F} \mid \|f\|_{\mathcal{F}} \leq t\}$; or \mathcal{F}_t could be designed sequentially by concatenating $\lfloor t \rfloor$ features together. This study will notably consider \mathcal{F}_t to be a space of polynomials of degree less than $\lfloor t \rfloor$, together with a partition of the input space; or \mathcal{F}_t associated with $\lambda_t^{-1} k_{\sigma_t}$ for a base kernel k_σ and λ_t, σ_t decreasing with t . Given a family (\mathcal{F}_t) , and a number of samples n , the optimal $t = t(n)$ to define $f_n = f_{n,1}$ according to (5) or (6) is found by balancing the variance $\varepsilon^2 \mathcal{N}(t)/n$ and the bias term $\lambda_t^2 \mathcal{S}(t)$. Note that $t(n)$ might not be known in practice, but could be tuned through cross validation.

3 A closer look on Taylor, Fourier or wavelet expansions estimation

The crux of this paper is to state that rates derived through Theorem 2 are only meaningful when one has enough samples, so to be able to consider function space \mathcal{F}_t containing interesting-enough functions with still having more samples than the effective dimension of \mathcal{F}_t . To this end, this section shows how the constants that appear in front of $n^{-2\alpha/(2\alpha+d)}$ in Theorem 1 are expected to be exponential in the dimension.

3.1 Taylor and local polynomial estimators

A natural idea to estimate a target function that is known to be regular, e.g. $f^* \in C^\alpha$ with C^α the space of α -Hölder functions, is to estimate its Taylor expansion with localized polynomials. It is well-known that this method will guarantee convergence rates in $O(n^{-2\alpha/(2\alpha+d)})$ as per Theorem 1, a fact that can be proved with Theorem 2 as detailed in Appendix A.4.1.

For ridge-less regression with adaptive algorithms, the length of the transitory regimes (that reflects in the constants inside the big O s) can be thought as lower bounded by the number of samples needed to match the effective dimension of the smallest class of functions that contains the target function (think of the smallest n that solves the equation $\mathcal{N}(t(n))/n \leq 1$ under the constraint $f^* \in \mathcal{F}_{t(n)}$). With a strong prior on f^* , one could take $\mathcal{F}_{t(n)} = \mathbb{R} \cdot f^*$ and cast the learning f^* as a one dimensional problem, which would require only one sample in the noiseless case. Without strong priors, a more natural algorithm would consider \mathcal{F}_t to be all polynomials of degree smaller than $\lfloor t \rfloor$, and adapt the degree so to be able to learn any f^* as per Stone-Weierstrass approximation theorem. Hence, assuming that f^* is orthogonal to all polynomials of degree smaller than s , so that no learning can take place before reaching $t(n) = s$, the number of samples needed to start learning

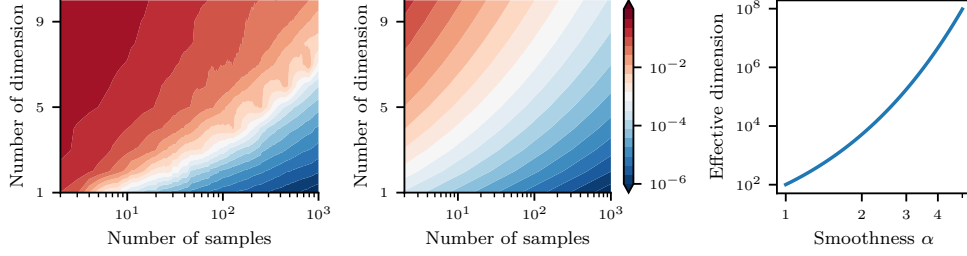


Figure 2: (Left) Convergence rates as a function of the input dimension d and the number of samples n when the target function is $f^*(x) = x_1^5$ and $k(x, y) \propto (1 + x^\top y)^5$. (Middle) Theoretical lower bound. We see a transitory regime when the number of samples is small in comparison with the dimension of the input space, hence the effective dimension of the model, which is $\binom{d+5}{5}$. (Right) Illustration of $\mathcal{N}(\alpha) = \binom{d+\alpha}{\alpha}$ for $d = 100$, which corresponds to the dimension of the space of polynomials with d variables of degree at most α . Given a number of samples, Taylor expansion can only be estimated meaningfully up to a certain order, e.g. when $n = 10^6$, one needs $\alpha \leq 4$ to ensure to have as many samples as unknown in the Taylor expansion of order α . See Appendix C.2 for details.

with Taylor expansion is of the same order as the number of coefficients in a polynomial of degree s . The following theorem, illustrated on Figure 2, offers a pessimistic view on this number and the consequent learning limit.

Proposition 1 (Taylor expansion learning limit). *When $\rho_{\mathcal{X}}$ is uniform on $[0, 1]^d$ and $f^* \in C^\alpha$ is estimated with Taylor expansions up to degree α (a.k.a. local polynomials), we have*

$$\frac{\varepsilon^2 \mathcal{N}_2(0)}{n} + \mathcal{B}(0) \geq \binom{d + \alpha}{\alpha} \frac{\varepsilon^2}{n}. \quad (11)$$

3.2 Fourier and translation-invariant kernels

Rather than local properties, one could leverage global smoothness properties, such as fast decays of Fourier coefficients, e.g. $f^* \in H^\alpha$ with H^α the Sobolev space of functions that are α -times differentiable with derivatives in $L^2(\rho_{\mathcal{X}})$. In this context, one can guarantee minimax convergence rates in $O(n^{-2\alpha/(2\alpha+d)})$ as per Theorem 1 with Fourier coefficient estimators, which are implicitly built from translation-invariant kernels, i.e. $k(x, x') = q((x - x')/\sigma)$ for $q : \mathbb{R}^d \rightarrow \mathbb{R}$ and σ a bandwidth parameter, as detailed in Appendix A.4.2.

At a high level, Fourier expansion can be seen as polynomial expansion in Fourier domain, where the number of frequencies (i.e. trigonometric monomials $x \mapsto e^{im^\top x}$ with $m \in \mathbb{Z}^d$) smaller than a cut-off frequency ($\|m\| < m_0$) grows exponentially with the dimension. As a consequence, similarly to Proposition 1, the number of points needed to discriminate between functions with frequencies smaller than m_0 will scale exponentially with the dimension. However, a key difference here is due to the presence of the regularization parameter λ : while local polynomial estimators strictly forbid the use of high-order polynomials, Fourier coefficient estimators only penalize the use of high frequencies. The following proposition offers a learning limit in a simple “harmonic setting”. More complicated settings can be shown as behaving similarly up to “interpolation” constants.

Proposition 2. *For the Matérn kernel corresponding to $\mathcal{F} = H^\beta$, on the torus $\mathbb{T}^d = \mathbb{R}^d/\mathbb{Z}^d$ with uniform measure $\rho_{\mathcal{X}}$, when $f^* : x \mapsto \cos(2\pi m^\top x)$ is a function with a single frequency $m \in \mathbb{Z}^d$,*

$$\inf_{\lambda > 0} \frac{\varepsilon^2 \mathcal{N}_2(\lambda)}{n} + \lambda^2 \mathcal{S}(\lambda) \geq \max_{l \in [d]} \left(\frac{l \pi^{(l-1)/2} \varepsilon^2}{2^{l-1} \Gamma((l-1)/2) n} \right)^\gamma (1 + \|m\|^2)^{\gamma l/2},$$

where $\gamma = 4\beta/(4\beta + l)$ goes to one as β goes to infinity.

In view of Proposition 2, for a frequency $m \in \mathbb{Z}^d$ with $\|m\| = m_0$ fixed, constants in front of convergence rates in Theorem 1 will start growing exponentially as the dimension increases, which we illustrate empirically on Figure 7.

Kernel	\mathcal{F}	$\mathcal{N}(\sigma, \lambda)$	$\mathcal{B}(\sigma, \lambda; H^\alpha)$
Gaussian	$\mathcal{F} \subset C^\omega$	$\sigma^{-d} \log(\lambda^{-1} \sigma^d)^{d/2}$	$\sigma^{2\alpha} \log(\lambda^{-1} \sigma^d)^{-\alpha}$
Matérn	H^β	$\sigma^{-d(2\beta-d)/2\beta} \lambda^{-d/2\beta}$	$\sigma^{(2\beta-d)\alpha/\beta} \lambda^{\alpha/\beta}$
Exponential	$H^{(d+1)/2}$	$(\sigma\lambda)^{-d/(d+1)}$	$(\sigma\lambda)^{2\alpha/(d+1)}$

Table 1: Example of translation-invariant kernels, their associated function classes, upper bounds (up to multiplicative constants) on their sizes as a function of the bandwidth σ and regularization parameter λ , as well as on the bias when approximating a function in the Sobolev space H^α . See Appendix B for details.

3.3 Wavelets and abstract RKHS expansions

Just like localized polynomial expansions (giving rise to Taylor expansions), one could consider localized Fourier expansions. This can be done in a relatively efficient way with wavelet expansions. The theory of wavelets offers a framework to separate the reconstruction of a target function at different scales and at different locations. A wavelet-oriented RKHS would be associated with a basis of wavelet functions $f_{\omega,x}$, ω being a frequency and x a localization parameter, and a norm defined as

$$\|f\|_{\mathcal{F}}^2 = \sum_{\omega \in \mathbb{Z}_+} \sum_{x \in \mathbb{Z}^d, \|x\| \leq \omega} q_{\omega,x}^{-1} \langle f, f_{\omega,x} \rangle^2,$$

for some suitably decaying coefficients $q_{\omega,x}$. In a stylized settings where the $f_{\omega,x}$ are orthogonal in $L^2(\rho)$, they would diagonalize the operator K , with associated eigenvalues $q_{\omega,x}$. Since the difficulty of estimating a target function f^* is directly linked to its norm $\|f^*\|_{\mathcal{F}} = \|K^{-1/2} f\|_{L^2(\rho_X)}$, the difficulty of learning $f_{\omega,x}$ would be associated with $q_{\omega,x}$, in the sense that $q_{\omega,x}$ would appear as an explicit constant in lower bounds. Assuming without restriction that K has been normalized to have unit trace, if some localization invariance enforces $q_{\omega,x} = q_\omega$, we would have

$$1 = \mathbb{E}_{X \sim \rho_X} [k(X, X)] = \text{Tr } K = \sum_{\omega \in \mathbb{Z}_+} \sum_{x \in \mathbb{Z}^d, \|x\| \leq \omega} q_{\omega,x} \gtrsim \sum_{\omega \in \mathbb{Z}_+} \omega^{d-1} q_\omega d\omega,$$

which implies that q_ω should decrease exponentially fast with respect to the dimension. Hence for a fixed ω , as the input dimension increases, the difficulty to learn a $f_{\omega,x}$ will grow exponentially fast.¹ The high-level picture is quite simple: given a kernel K , one has a fixed “estimation ability” budget ($\text{Tr } K$) to allocate to different functions (the $f_{\omega,x}$ through $q_{\omega,x}$); as the number of dimensions increases, there are exponentially more regular functions (e.g. frequencies of norm ω), making them exponentially harder to estimate, and increasing exponentially the number of samples needed to reach the final convergence rate regime.

4 Exploring transitory regimes

In the preceding paragraphs, we have seen how rates in $O(n^{-2\alpha/(2\alpha d)})$ might take time to appear in practice on figures that plot the generalization error against the number of samples. Interestingly, the classical analysis can be retaken and slightly modified to describe transitory regimes that might appear on those plots as long as we stay in high-sample regimes where $\mathcal{N}(\lambda) < n$. This section presents such an analysis, as well as numerical experiments to explore the low-sample regimes missing from our theoretical analysis.

4.1 Theoretical analysis of high-samples regimes

We begin by a proposition in a stylized setting, which provides a complete picture of the size of usual reproducing kernel Hilbert spaces formed by Sobolev spaces, as well as their adherence to other Sobolev spaces.

¹Note that, to make this formal, one would have to make sure, as we did in Proposition 2, that the constant appearing in the effective dimension does not counterbalance the $\|f_{\omega,x}\|^2$ constant.

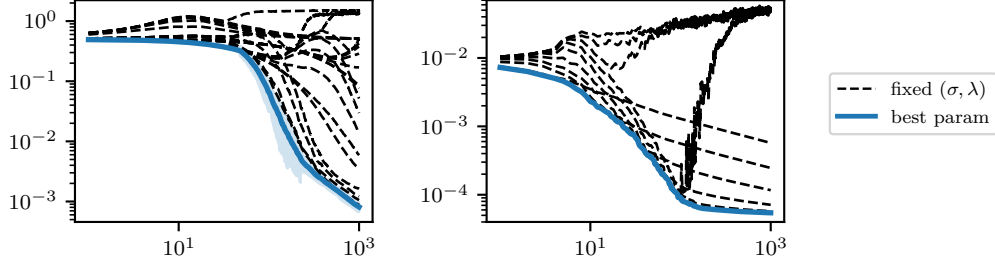


Figure 3: Composite convergence rates profile. The x -axis corresponds to the number of samples, while the y -axis corresponds to the excess risk. From the analysis in Section 4.1, one can build different convergence rates profiles. For example, regular functions with relatively high-frequencies are going to be hard to learn with few samples but really easy after a certain number of samples, roughly equals to the number of harmonics with lower-frequencies; while regular low-frequency functions with singularity are going to show convergence rates where the coarse details of the functions are learned with few samples, but the reconstructions of fine-grained details will required much more samples. The former profile is illustrated with the left figure, and the latter on the right figure. For any sample sizes, excess risk is reported for the best hyperparameters, found with cross-validation. More details are provided in Appendix C.3.

Proposition 3 (Capacity and bias bounds). *When $\rho_{\mathcal{X}}$ is uniform on the torus $\mathbb{T}^d = \mathbb{R}^d / \mathbb{Z}^d$, and k is a translation-invariant kernel $k(x, y) = q((x - y)/\sigma)$, the capacity of the space defined through k with regularization λ and bandwidth σ verifies, for $a \in \{1, 2\}$,*

$$\mathcal{N}_a(\sigma, \lambda) = \int_{\mathbb{R}^d} \left(\frac{\hat{q}(\sigma\omega)}{\hat{q}(\sigma\omega) + \lambda\sigma^{-d}} \right)^a \#(d\omega), \quad (12)$$

where $\#$ is the counting measure on $\mathbb{Z}^d \subset \mathbb{R}^d$, and \hat{q} is the (discrete) Fourier transform of q . Similarly, the biases quantifying the adherence of f^* in \mathcal{F} verify

$$\mathcal{S}(\sigma, \lambda) = \int_{\mathbb{R}^d} \frac{|\hat{f}^*(\omega)|^2}{(\sigma^d \hat{q}(\sigma\omega) + \lambda)^2} \#(d\omega). \quad (13)$$

Moreover on $\mathcal{X} = \mathbb{R}^d$, if $\rho_{\mathcal{X}}$ has a density bounded above by $\rho_{\infty} < +\infty$, then (12) and (13) become inequalities for μ the Lebesgue measure and \hat{f} the continuous Fourier transform, at the cost of extra constants in front of their right-hand sides (respectively ρ_{∞} and $\max(\rho_{\infty}, 1)$ for \mathcal{N}_a and \mathcal{S}).

Proposition 3 unlocks a precise sense of the effective dimension for the Gaussian kernel, defined with $q(x) = \exp(-\|x\|^2)$, the exponential kernel, with $q(x) = \exp(-\|x\|)$, and the Sobolev kernel, with $\hat{q}(\omega) = (1 + \|\omega\|^2)^{-\beta}$, as well as the bias term $\mathcal{S}(H^{\alpha})$ when approximating a function $f \in H^{\alpha}$ with those kernels. This is reported in Table 1 and proved in Appendix B. Moreover, the linearity of the bias formulation in Proposition 3 is theoretically useful to decorrelate the estimation of different power laws appearing in the Fourier transform of f . More precisely, if

$$|\hat{f}^*(\omega)|^2 = \int_{\alpha}^{\infty} c_{\gamma} (1 + \|\omega\|^2)^{-\gamma} \mu(d\gamma),$$

with c_{γ} the inverse of the constant in front of the upper bound for $\lambda^2 \mathcal{S}(H^{\gamma})$ in Table 1, and μ some measure with a profile that ensures the good definition of $f^* \in H^{\alpha}$, we have, taking for example k as the Gaussian kernel,

$$\lambda^2 \mathcal{S}(\sigma, \lambda; f^*, k) \simeq \int_{\alpha}^{\infty} (\sigma^2 \log(\lambda^{-1} \sigma^d)^{-1})^{\gamma} \mu(d\gamma).$$

In particular, with $\sigma^2 \log(\lambda^{-1} \sigma^d)^{-1} = n^{-r}$, we get the following convergence rate profile:

$$\mathbb{E}_{\mathcal{D}_n}[\mathcal{E}(f_n)] \lesssim \inf_{r \in \mathbb{R}} n^{-1+rd/2} + \int_{\alpha}^{\infty} n^{-\gamma r} \mu(d\gamma). \quad (14)$$

This characterization enables us to easily create target functions exhibiting different convergence profiles, as long as we stay in the high-sample regimes where our bounds are meaningful. The following examples illustrate how, given a target function and a range on the number of available samples, convergence behaviors might fall in regimes that do not correspond to the steady convergence rate in $O(n^{-2\alpha/2\alpha+d})$ predicted by Theorem 1.

- *Slow then fast profile.* The first type of profile that can be created is for functions that are supported on a few eigenfunctions of K associated with small eigenvalues. A typical example of this profile in one dimension would be $f^*(x) = \cos(\omega x)$ for a high frequency ω . For this target function, no meaningful learning can be done when the search space is too small, because small search spaces do not contain high-frequency functions. On the other hand, when the search space is big enough, the bias quickly goes to zero, allowing for fast learning as long as one controls the estimation error. When provided with few samples, one would prefer a small search space to avoid blowing up of the estimation error, and learning will stall until enough samples are collected to explore bigger search spaces, where f^* could be learned quickly. We illustrate this profile on Figure 3.
- *Fast then slow profile.* The second type of profile is built from μ that charges most of its mass on fast decays, but also puts some small mass on slow decays. It corresponds to target functions that are roughly well approximated by highly smooth functions, but whose exact reconstruction needs to incorporate less regular functions. The smooth part of the function will be learned quickly, yet the non-smooth part will be learned slowly. Typical examples of such a profile are provided by non-smooth functions that can be turned into infinitely differentiable ones after introducing infinitesimal perturbations, such as $f^*(x) = \exp(-\min(|x|^2, M))$, which is only C^0 , but where one can expect to learn fast before stalling to estimate the C^1 -singularity. Another example is given by a function made of a sum of one low-frequency cosine with large amplitude easy to learn together with one high-frequency cosine with small amplitude much harder to learn. We illustrate these profiles on Figure 3.

4.2 Empirical study of low-sample regimes.

In this work, we have focused on “under-parameterized” situations where the parameters were set to have more samples than the effective dimension of the resulting functional space $\mathcal{F}_{t(n)}$. In a deep learning world, where many phenomena are understood as taking place in the “over-parameterized” regime, it is of interest to compare our perspective with the double descent phenomenon. Figure 1 shows the excess risk as a function of two of the three parameters (n, σ, λ) , as well as the graph defined by $\{(n, \sigma, \lambda) \mid \mathcal{N}_1(\lambda, \sigma) = n\}$. It illustrates a double descent phenomena with “phase” transition governed by the passage from the low-sample to the high-sample regime. Figure 12 tries to explain this phenomena by looking at weights $\hat{\alpha}_X$ satisfying $\mathbb{E}_{\mathcal{D}_n}[f_{n,\lambda}(x)] = \mathbb{E}_{(X,Y)}[\hat{\alpha}_X(x)Y]$, and whose closed form is given in Appendix C.4. The attentive reader will note that this double descent phenomenon takes place in the regularized setup, and not in the interpolation regime, contrarily to prior works on the matter [e.g. 26, 19]. Experiments are detailed in Appendix C.

5 Conclusion

In this paper, we have shown how subtle is the saying that smoothness allows to break the curse of dimensionality. In particular, if smoothness is leveraged through Taylor expansions, the number of samples needed to leverage the existence of a good approximation of the target function by polynomials of degree α grows as $\binom{d+\alpha}{d}$, making it prohibitive in high dimensions. When smoothness is leveraged through Fourier (or wavelet) expansions, the picture is slightly different, and the required sample size is linked with a Fourier-based (or wavelet-based) norm of the target function, and since the number of functions of a fixed regularity increases exponentially fast with the input dimension, so does the norm of those functions, and the need for samples to guarantee a given excess risk.

Future work. Since we have shown that smoothness alone is not a strong enough prior to build efficient learning algorithms in high-dimensions, other priors could be investigated. As such, sparsity

assumptions, multi-index models, feature learning or multi-scale behaviors might offer more realistic models to break the curse of dimensionality. How deep learning models exploit such priors has been an active line of research, although linking theoretical results with “interpretable” observations in neural networks remains challenging, and theory has not yet provided that many meaningful insights for practitioners.

Furthermore, going beyond the sole selection of a few hyperparameters, it would be interesting to understand more aggressive model selection. In particular, given some observations (X_i, Y_i) and some hypothesis classes \mathcal{F}_t , it seems natural to trade a term that fits the data as per (5), together with a regularization term $\lambda \min_t \|f\|_{\mathcal{F}_t}$ that selects \mathcal{F}_t so that f_n has a small \mathcal{F}_t norm. We understand this as a *lex parsimoniae*, where each \mathcal{F}_t encodes different notions of simplicity (e.g. different priors) while f_n only needs to satisfy one of them.

Finally, while this work heavily relies on the least-square loss, practitioners tend to favor other losses such as the cross-entropy. How losses deform and modify the size of the search space \mathcal{F} and its adherence properties to some target functions f^* is an open-question –not to mention its adherence properties when the final predictor is built as a decoding $y(x) = \arg \max_y f(y|x)$ in order to learn a discrete y from a score $f(y|x)$ that relates to $\mathbb{P}_{(X,Y) \sim \rho}(Y = x | X = x)$.

Experiments reproduction. All the code to run figures is available at <https://github.com/VivienCabannes/rates>.

Acknowledgements. VC would like to thank Alberto Bietti, Jaouad Mourtada and Francis Bach for useful discussions.

References

- [1] Robert Adams and John Fournier. *Sobolev Spaces*. Academic Press, 1975.
- [2] Nachman Aronszajn. Theory of reproducing kernels. *Transactions of the American Mathematical Society*, 1950.
- [3] Francis Bach. High-dimensional analysis of double descent for linear regression with random projections. *arXiv preprint arXiv:2303.01372*, 2023.
- [4] Francis Bach. *Learning Theory from First Principles*. MIT press (announced), 2023.
- [5] Vivien Cabannes, Alessandro Rudi, and Francis Bach. Fast rates in structured prediction. In *Conference on Learning Theory*, 2021.
- [6] Andrea Caponnetto and Ernesto De Vito. Optimal rates for the regularized least-squares algorithm. *Foundations of Computational Mathematics*, 2006.
- [7] William Cleveland. Robust locally weighted regression and smoothing scatterplots. *Journal of the American Statistical Association*, 1979.
- [8] Luc Devroye, László Györfi, and Gábor Lugosi. *A probabilistic theory of pattern recognition*. Springer, 2013.
- [9] Simon Fischer and Ingo Steinwart. Sobolev norm learning rates for regularized least-squares algorithms. *Journal of Machine Learning Research*, 2020.
- [10] Evelyn Fix and Joseph Hodges. Discriminatory analysis. Nonparametric discrimination: Consistency properties. Technical report, School of Aviation Medicine, Randolph Field, Texas, 1951.
- [11] László Györfi, Michael Kohler, Adam Krzyżak, and Harro Walk. *A Distribution-Free Theory of Nonparametric Regression*. Springer, 2002.
- [12] Andrey Kolmogorov and Vladimir Tikhomirov. ε -entropy and ε -capacity of sets in functional spaces. *Uspekhi Matematicheskikh Nauk*, 1979.

- [13] Tengyuan Liang and Alexander Rakhlin. Just interpolate: Kernel “ridgeless” regression can generalize. *The Annals of Statistics*, 2020.
- [14] Song Mei and Andrea Montanari. The generalization error of random features regression: Precise asymptotics and the double descent curve. *Communications on Pure and Applied Mathematics*, 2022.
- [15] Song Mei, Theodor Misiakiewicz, and Andrea Montanari. On the estimation of the derivatives of a function with the derivatives of an estimate. *Applied and Computational Harmonic Analysis*, 2022.
- [16] Jaouad Mourtada and Lorenzo Rosasco. An elementary analysis of ridge regression with random design. *Comptes Rendus. Mathématique*, 2022.
- [17] Jaouad Mourtada, Tomas Vaškevičius, and Nikita Zhivotovskiy. Distribution-free robust linear regression. *Mathematical Statistics and Learning*, 2022.
- [18] Jaouad Mourtada, Tomas Vaškevičius, and Nikita Zhivotovskiy. Local risk bounds in statistical aggregation. *Preprint*, 2023.
- [19] Nicolò Pagliana, Alessandro Rudi, Ernesto De Vito, and Lorenzo Rosasco. Interpolation and learning with scale dependent kernels. In *ArXiv*, 2020.
- [20] Jaak Peetre. New thoughts on Besov spaces. *Duke University Mathematics Series*, 1976.
- [21] Alexander Rakhlin and Xiyu Zhai. Consistency of interpolation with laplace kernels is a high-dimensional phenomenon. In *Conference on Learning Theory*, 2019.
- [22] Carl Rasmussen and Christopher Williams. *Gaussian Processes for Machine Learning*. The MIT Press, 2005.
- [23] Bernhard Scholkopf and Alexander Smola. *Learning with kernels: support vector machines, regularization, optimization, and beyond*. MIT press, 2001.
- [24] Steve Smale and Ding-Xuan Zhou. Estimating the approximation error in learning theory. *Analysis and Applications*, 2003.
- [25] Steve Smale and Ding-Xuan Zhou. Learning theory estimates via integral operators and their approximations. *Constructive Approximation*, 2007.
- [26] Stefano Spigler, Mario Geiger, Stéphane d’Ascoli, Levent Sagun, Giulio Biroli, and Matthieu Wyart. A jamming transition from under- to over-parametrization affects loss landscape and generalization. *Journal of Physics A: Mathematical and Theoretical*, 2019.
- [27] Charles Stone. Consistent nonparametric regression. *The Annals of Statistics*, 1977.
- [28] Hans Triebel. *Interpolation Theory, Function Spaces, Differential Operators*. North-Holland Publishing Co., 1978.
- [29] Vladimir Vapnik. *The Nature of Statistical Learning Theory*. Springer, 1995.
- [30] Ding-Xuan Zhou. The covering number in learning theory. *Journal of Complexity*, 2002.

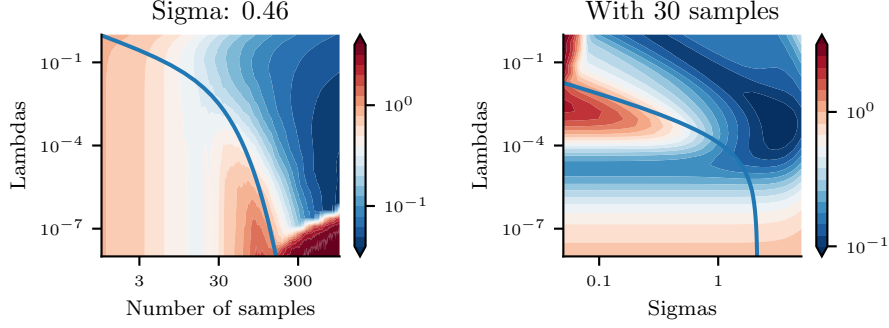


Figure 4: Two other cuts of Figure 1.

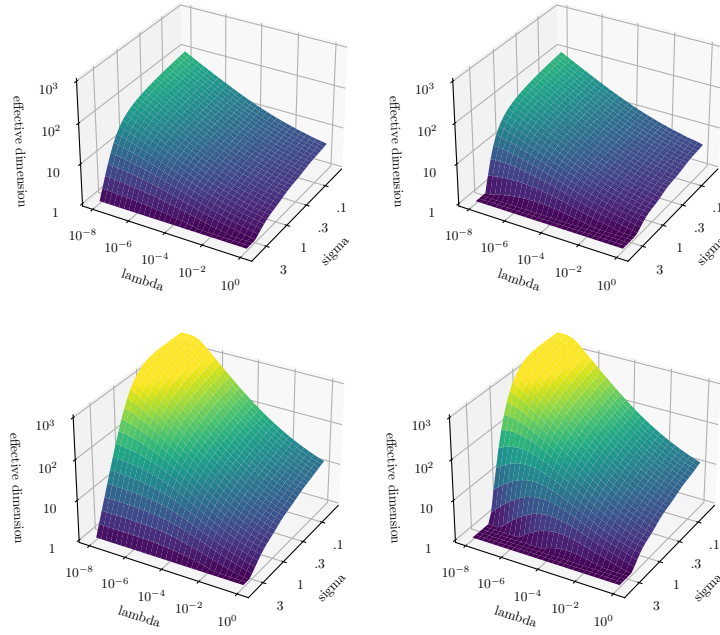


Figure 5: Effective dimensions \mathcal{N}_1 (left) and \mathcal{N}_2 (right) as a function of (λ, σ) in one dimension (top) and two dimension (bottom) when $\rho_{\mathcal{X}}$ is uniform on $\mathcal{X} = [-1, 1]^d$, and k is the Gaussian kernel.

A Generic proofs and discussions

A.1 What do we mean by transitory regimes?

In essence, by transitory regimes we mean any finite-time behavior that does not match an expected long-time horizon “stationary” behavior. More precisely, let $\Gamma = \{(n, \mathbb{E}_{\mathcal{D}_n}[\mathcal{E}(f_n)]) \mid n \in \mathbb{N}\}$ be the graph of the expected excess risk. Theorem 2 provides a lower-upper bound of the form $\Gamma \subset \{(n, cn^{-\gamma}(1 + ah(n))) \mid n \in \mathbb{N}, a \in [-1, 1]\}$ with c, γ two constants and h a function that goes to zero when its argument goes to infinity. This shows that, as n grows large, $\mathbb{E}_{\mathcal{D}_n}[\mathcal{E}(f_n)]$ will behave as $cn^{-\gamma}$. However, this stationary behavior in $cn^{-\gamma}$ might take time to kick in, and when only accessing a small number of samples n , our bound does not lead to strong constraints on $\mathbb{E}_{\mathcal{D}_n}[\mathcal{E}(f_n)]$, which might arguably exhibit a very different profile. We illustrate this idea on Figure 6.

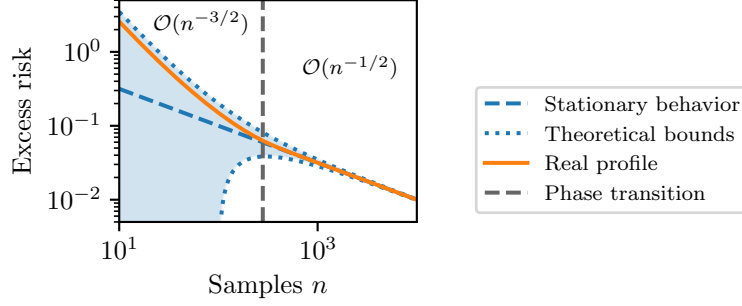


Figure 6: Illustration of transitory regimes. In essence, Theorem 2 states that $\mathcal{E}_n := \mathbb{E}_{\mathcal{D}_n}[\mathcal{E}(f_{n,\lambda})] = A(n, \lambda)(1 + h(n, \lambda))$ for $h = O(\mathcal{N}_\infty(\lambda)/n)$. We illustrate our upper-lower bound when $A(n, \lambda_n) = n^{-1/2}$ and $nh(n, \lambda_n)$ is known to be in $[-10^2, 10^2]$. The upper-lower bound forces \mathcal{E}_n to behave in $n^{-1/2}$ when n goes to infinity, yet when n is small, it can showcase quite different “transitory” behaviors.

A.2 Regularization is a change of kernel

Kernel ridge regression (6) with a kernel k_1 and a regularization parameter λ_1 is equivalent to kernel ridge regression with a kernel $k_2 = \lambda_1^{-1}k_1$ and a regularization parameter $\lambda_2 = 1$. Indeed, In the definition of the regularized risk (6), the regularization parameter λ and the kernel k only appear in one term $\lambda \|f\|_{\mathcal{F}}$. This term can be written as

$$\lambda \langle f, K^{-1}f \rangle_{L^2(\rho)} = \langle f, (\lambda^{-1}K)^{-1}f \rangle_{L^2(\rho)}.$$

Because K depends linearly on k , $\lambda^{-1}K$ is the integral operator linked with the kernel $\lambda^{-1}k$ when k is the kernel associated with the operator K .

The interpolation setting where $\lambda_1 = 0$ but f is searched in $\mathcal{F} = \text{im } K^{1/2}$ corresponds to the barrier regularization $\chi_{\mathcal{F}}$, where $\chi_A(x) = 0$ in $x \in A$ and $+\infty$ otherwise. In other terms, the limiting case where $\lambda_1 = 0$ corresponds to kernel ridge regression with $\lambda_2 = 1$, $\|f\|_{\mathcal{F}_2} = +\infty$ if $f \notin \mathcal{F}_2$ and zero otherwise.

A.3 Excess risk bounds - Proof of Theorem 2 and corollaries

For ease of notation, we will use the finite-dimensional notation $u^\top w$ also to denote the inner product $\langle u, v \rangle$ in (infinite-dimensional) Hilbert spaces. Moreover, we will simply write $\|\cdot\|$ for both $\|\cdot\|_{\mathcal{H}}$ and the operator norm on \mathcal{H} (depending on context), L^2 for $L^2(\rho_{\mathcal{X}})$, and $\|\cdot\|_2$ for both $\|\cdot\|_{L^2}$ and the operator norm on L^2 . While in our statements, for the sake of clarity, we have expressed everything in terms of operators on L^2 , for the proofs it is more convenient to work on \mathcal{H} . Let us introduce the embedding

$$S : \mathcal{H} \rightarrow L^2, \quad \theta \mapsto (x \mapsto \theta^\top \varphi(x)).$$

From S , one can take its adjoint S^* and check that $K = SS^*$. K is isometric to the (non-centered) covariance operator

$$\Sigma = S^*S = \mathbb{E}[\varphi(X) \otimes \varphi(X)].$$

Note that

$$\|S\theta\|_2^2 = \mathbb{E}[(\varphi(X)^\top \theta)^2] \leq \mathbb{E}[\|\varphi(X)\|^2 \|\theta\|^2] = \|\varphi\|_2^2 \|\theta\|^2,$$

which implies that K is a continuous operator as soon as $\varphi \in L^2$. The kernel ridge regression estimator (6) is characterized as

$$f_n = S(\Sigma_n + \lambda)^{-1}S_n^*\mathbb{Y},$$

where

$$S_n : \mathcal{H} \rightarrow \mathbb{R}^n, \quad \theta \mapsto (\theta^\top \varphi(X_i))_{i \in [n]}, \quad \Sigma_n = S_n^*S_n, \quad \mathbb{Y} = (Y_i)_{i \in [n]} \in \mathbb{R}^n.$$

Endowing \mathbb{R}^n with the scalar product $\langle a, b \rangle = \frac{1}{n} \sum_{i \in [n]} a_i b_i$, we have

$$S_n^* \mathbb{Y} = \frac{1}{n} \sum_{i \in [n]} Y_i \varphi(X_i), \quad \Sigma_n = \frac{1}{n} \sum_{i=1}^n \varphi(X_i) \otimes \varphi(X_i).$$

It is useful to define ε_i as the difference between Y_i and $f^*(X_i) = \mathbb{E}[Y_i | X = X_i]$, which can be seen as the labeling noise and average to zero. We have, with $E = (\varepsilon_i)_{i \in [n]} \in \mathbb{R}^n$,

$$Y_i = f^*(X_i) + \varepsilon_i = \varphi(X_i)^\top \theta_* + \varepsilon_i, \quad \mathbb{Y} = S_n \theta_* + E.$$

As a consequence,

$$f_n = S(\Sigma_n + \lambda)^{-1} \Sigma_n \theta_* + S(\Sigma_n + \lambda)^{-1} S_n^* E.$$

Let $\mathbb{X} = (X_i)_{i \in [n]}$. When our model is well specified so that $f^* = S\theta_*$, we have

$$\begin{aligned} \mathbb{E}_{\mathcal{D}_n} [\mathcal{E}(f_n) | \mathbb{X}] &= \mathbb{E}_{\mathcal{D}_n} [\|f_n - f^*\|_2^2 | \mathbb{X}] \\ &= \|S(\Sigma_n + \lambda)^{-1} \Sigma_n \theta_* - S\theta_*\|_2^2 \\ &\quad + \mathbb{E}_{\mathcal{D}_n} [\|S(\Sigma_n + \lambda)^{-1} S_n^* E\|_2^2 | \mathbb{X}] \\ &\quad + 2\mathbb{E}_{\mathcal{D}_n} [(S(\Sigma_n + \lambda)^{-1} \Sigma_n \theta_* - S\theta_*)^\top S(\Sigma_n + \lambda)^{-1} S_n^* E | \mathbb{X}] \\ &= \lambda^2 \|S(\Sigma_n + \lambda)^{-1} \theta_*\|_2^2 \\ &\quad + \mathbb{E}_{\mathcal{D}_n} [\|S(\Sigma_n + \lambda)^{-1} S_n^* E\|_2^2 | \mathbb{X}] \\ &\quad + 2 (S_n(\Sigma_n + \lambda)^{-1} \Sigma(\Sigma_n + \lambda)^{-1} \theta_*)^\top \mathbb{E}_{\mathcal{D}_n} [E | \mathbb{X}] \\ &= \lambda^2 \|S(\Sigma_n + \lambda)^{-1} \theta_*\|_2^2 + \mathbb{E}_{\mathcal{D}_n} [\|S(\Sigma_n + \lambda)^{-1} S_n^* E\|_2^2 | \mathbb{X}], \end{aligned}$$

where in the third equality we used $I - (\Sigma_n + \lambda)^{-1} \Sigma_n = \lambda(\Sigma_n + \lambda)^{-1}$, and in the last one $\mathbb{E}_{\mathcal{D}_n} [E | \mathbb{X}] = 0$. Assuming for simplicity that the noise is homoscedastic so that $\mathbb{E}[EE^\top] = \varepsilon^2 I$ for $\varepsilon > 0$, we obtain

$$\begin{aligned} \mathbb{E}_{\mathcal{D}_n} [\|S(\Sigma_n + \lambda)^{-1} S_n^* E\|_2^2 | \mathbb{X}] &= \frac{1}{n} \text{Tr} (S_n(\Sigma_n + \lambda)^{-1} \Sigma(\Sigma_n + \lambda)^{-1} S_n^* \mathbb{E}_{\mathcal{D}_n} [EE^\top | \mathbb{X}]) \\ &= \frac{\varepsilon^2}{n} \text{Tr} (\Sigma(\Sigma_n + \lambda)^{-2} \Sigma_n), \end{aligned}$$

where the $1/n$ factor arises from the fact that $E^* = E^\top/n$ in the geometry we have considered on \mathbb{R}^n . Finally we have retrieved the following standard bias-variance decomposition result.

Lemma 4 (Bias-Variance decomposition). *When our model is well-specified so that $f^* = S\theta_*$ with $\theta_* \in \mathcal{H}$, and when the noise in the label is homoscedastic with variance ε^2 , the estimator (6) verifies*

$$\mathbb{E}_{\mathcal{D}_n} [\mathcal{E}(f_n) | \mathbb{X}] = \underbrace{\lambda^2 \|S(\Sigma_n + \lambda)^{-1} \theta_*\|_2^2}_{\mathcal{B}_n} + \underbrace{\frac{\varepsilon^2}{n} \text{Tr} (\Sigma(\Sigma_n + \lambda)^{-2} \Sigma_n)}_{\mathcal{V}_n}. \quad (15)$$

We would like to get the limit when n goes to infinity in equation (15). We expect the first term to concentrate towards $\lambda^2 \|S(\Sigma + \lambda)^{-1} \theta_*\|_2^2$, and the second term to $\text{Tr}(\Sigma^2(\Sigma + \lambda)^{-2})$.

A.3.1 Bounding the bias term

Let us begin by working out the term $\mathcal{B}_n = \|S(\Sigma_n + \lambda)^{-1} \theta_*\|_2^2$. We first introduce some notation to make derivations shorter. Let $E_n = \Sigma_n - \Sigma$, $\Sigma_\lambda = \Sigma + \lambda$ and $F_n = -\Sigma_\lambda^{-1/2} E_n \Sigma_\lambda^{-1/2}$. As long as

$\|F_n\| < 1$, we have

$$\begin{aligned}
\mathcal{B}_n &= \theta_*^\top (\Sigma_n + \lambda)^{-1} \Sigma (\Sigma_n + \lambda)^{-1} \theta_* \\
&= \theta_*^\top (\Sigma_\lambda + E_n)^{-1} \Sigma (\Sigma_\lambda + E_n)^{-1} \theta_* \\
&= \theta_*^\top \Sigma_\lambda^{-1/2} (I - F_n)^{-1} \Sigma_\lambda^{-1} \Sigma (I - F_n)^{-1} \Sigma_\lambda^{-1/2} \theta_* \\
&= \sum_{i,j \in \mathbb{N}} \theta_*^\top \Sigma_\lambda^{-1/2} F_n^i \Sigma_\lambda^{-1} \Sigma F_n^j \Sigma_\lambda^{-1/2} \theta_*.
\end{aligned}$$

Let us assume for a moment that

$$\left\| (\Sigma \Sigma_\lambda^{-1})^{-1/2} F_n (\Sigma \Sigma_\lambda^{-1})^{1/2} \right\| \leq \|F_n\|. \quad (16)$$

If equation (16) holds, then

$$\begin{aligned}
|\mathcal{B}_n - \theta_*^\top \Sigma_\lambda^{-2} \Sigma \theta_*| &= \left| \sum_{i,j \in \mathbb{N}; i+j \neq 0} \theta_*^\top \Sigma_\lambda^{-1/2} F_n^i \Sigma_\lambda^{-1} \Sigma F_n^j \Sigma_\lambda^{-1/2} \theta_* \right| \\
&\leq \sum_{i+j \neq 0} \left| \theta_*^\top \Sigma_\lambda^{-1/2} F_n^i \Sigma_\lambda^{-1} \Sigma F_n^j \Sigma_\lambda^{-1/2} \theta_* \right| \\
&= \sum_{i+j \neq 0} \left| \left\langle \Sigma_\lambda^{-1/2} (\Sigma_\lambda^{-1} \Sigma)^{1/2} \theta_*, \left((\Sigma_\lambda^{-1} \Sigma)^{-1/2} F_n^i \Sigma_\lambda^{-1} \Sigma F_n^j (\Sigma_\lambda^{-1} \Sigma)^{-1/2} \right) (\Sigma_\lambda^{-1} \Sigma)^{1/2} \Sigma_\lambda^{-1/2} \theta_* \right\rangle \right| \\
&\leq \sum_{i+j \neq 0} \left\| \Sigma_\lambda^{-1/2} (\Sigma_\lambda^{-1} \Sigma)^{1/2} \theta_* \right\|^2 \left\| (\Sigma_\lambda^{-1} \Sigma)^{-1/2} F_n^i \Sigma_\lambda^{-1} \Sigma F_n^j (\Sigma_\lambda^{-1} \Sigma)^{-1/2} \right\| \\
&= \theta_*^\top \Sigma_\lambda^{-2} \Sigma \theta_* \sum_{i+j \neq 0} \left\| ((\Sigma \Sigma_\lambda^{-1})^{-1/2} F_n (\Sigma \Sigma_\lambda^{-1})^{1/2})^{i+j} \right\| \\
&\leq \theta_*^\top \Sigma_\lambda^{-2} \Sigma \theta_* \sum_{i,j \in \mathbb{N}; i+j \neq 0} \left\| (\Sigma \Sigma_\lambda^{-1})^{-1/2} F_n (\Sigma \Sigma_\lambda^{-1})^{1/2} \right\|^{i+j} \\
&= \theta_*^\top \Sigma_\lambda^{-2} \Sigma \theta_* \sum_{i \in \mathbb{N}} (i+2) \left\| (\Sigma \Sigma_\lambda^{-1})^{-1/2} F_n (\Sigma \Sigma_\lambda^{-1})^{1/2} \right\|^{i+1} \\
&\leq \theta_*^\top \Sigma_\lambda^{-2} \Sigma \theta_* \sum_{i \in \mathbb{N}} (i+2) \|F_n\|^{i+1} \\
&= \theta_*^\top \Sigma_\lambda^{-2} \Sigma \theta_* \int_0^\infty (\lfloor x \rfloor + 2) \|F_n\|^{\lceil x \rceil} dx \\
&\leq \theta_*^\top \Sigma_\lambda^{-2} \Sigma \theta_* \int_0^\infty (x+2) \|F_n\|^x dx \\
&= \theta_*^\top \Sigma_\lambda^{-2} \Sigma \theta_* \frac{1 - 2 \log(\|F_n\|)}{\log^2(\|F_n\|)}.
\end{aligned}$$

This inequality is useful as long as $\|F_n\|$ is small enough, which is not always true. When $\|F_n\|$ is large, we can instead proceed with the simpler bound

$$|\mathcal{B}_n - \theta_*^\top \Sigma_\lambda^{-2} \Sigma \theta_*| \leq \mathcal{B}_n + \theta_*^\top \Sigma_\lambda^{-2} \Sigma \theta_* \leq 2 \theta_*^\top \Sigma \theta_* \lambda^{-2} = 2 \|f^*\|_2^2 \lambda^{-2}.$$

Therefore, rewriting the limit as

$$\begin{aligned}
\lambda^2 \theta_*^\top (\Sigma + \lambda)^{-2} \Sigma \theta_* &= \lambda^2 (\Sigma^{1/2} \theta_*)^\top (\Sigma + \lambda)^{-2} \Sigma^{1/2} \theta_* = \lambda^2 (S \theta_*)^\top (K + \lambda)^{-2} S \theta_* \\
&= \lambda^2 (f^*)^\top (K + \lambda)^{-2} f^* = \left\| \lambda (K + \lambda)^{-1} f^* \right\|_2^2 = \mathcal{B}(\lambda),
\end{aligned}$$

we split the bias error as

$$\begin{aligned} |\lambda^2 \mathcal{B}_n - \lambda^2 \theta_*^\top \Sigma_\lambda^{-2} \Sigma \theta_*| &\leq 2 \|f^*\|_2^2 \mathbf{1}_{\|F_n\| > 1/2} + \mathcal{B}(\lambda) \frac{1 - 2 \log(\|F_n\|)}{\log^2(\|F_n\|)} \mathbf{1}_{\|F_n\| \leq 1/2} \\ &\leq 2 \|f^*\|_2^2 \mathbf{1}_{\|F_n\| > 1/2} - \frac{3\mathcal{B}(\lambda)}{\log(\|F_n\|)} \mathbf{1}_{\|F_n\| \leq 1/2}. \end{aligned}$$

Taking the expectation and using the convexity of the absolute value, we obtain

$$|\mathbb{E}_{\mathcal{D}_n}[\lambda^2 \mathcal{B}_n] - \lambda^2 \theta_*^\top \Sigma_\lambda^{-2} \Sigma \theta_*| \leq 2 \|f^*\|_2^2 \mathbb{P}(\|F_n\| > 1/2) - \mathcal{B}(\lambda) \int_0^{1/2} \frac{3\mathbb{P}(\|F_n\| > x)}{\log(x)} dx.$$

We now proceed with an exponential concentration inequality on $\|F_n\|$. We will use the one of Cabannes et al. [5], Eq. (25). As long as $\lambda \leq \|\Sigma\|$, we have

$$\mathbb{P}(\|F_n\| > t) \leq 28\mathcal{N}_1(\lambda) \exp\left(-\frac{nt^2}{\mathcal{N}_\infty(\lambda)(1+t)}\right).$$

This inequality shows the restrictive notion of effective dimension, which is useful to ensure the good conditioning of the linear system implicitly encoded in (6), and, in essence, bound all moments of $\varphi(X)$. As long as $\mathcal{N}_\infty(\lambda) \leq 3n/2$, we can compute the integral as

$$\begin{aligned} -\int_0^{1/2} \frac{\mathbb{P}(\|F_n\| > x)}{\log(x)} dx &\leq -28\mathcal{N}_1(\lambda) \int_0^{1/2} \frac{\exp(-3nx^2/2\mathcal{N}_\infty(\lambda))}{\log(x)} dx \\ &= -28\mathcal{N}_1(\lambda) \frac{\mathcal{N}_\infty^{1/2}(\lambda)}{1.5^{1/2}n^{1/2}} \int_0^{1/2} \frac{\exp(-u^2)}{\log(u) + \log(3n/2\mathcal{N}_\infty^2(\lambda))} du \\ &\leq -28 \frac{\mathcal{N}_1(\lambda)\mathcal{N}_\infty^{1/2}(\lambda)}{1.5^{1/2}n^{1/2}} \int_0^{1/2} \frac{\exp(-u^2)}{\log(u)} du \leq \frac{8\mathcal{N}_1(\lambda)\mathcal{N}_\infty^{1/2}(\lambda)}{n^{1/2}}. \end{aligned}$$

We recall that the bounds above were derived under condition (16), which is rather strong. However, the attentive reader would remark that a much laxer assumption is sufficient, which we introduce thereafter.

Assumption 1. *There exists a constant c such that, for all $i, j \in \mathbb{N}$,*

$$\mathbb{E} \left[\left| (\Sigma \Sigma_\lambda^{-1})^{-.5} F_n^i \Sigma \Sigma_\lambda^{-1} F_n^j (\Sigma \Sigma_\lambda^{-1})^{-.5} \right| \mid \|F_n\| \leq 1/2 \right] \leq c^2 \mathbb{E} \left[\|F_n\|^{i+j} \mid \|F_n\| \leq 1/2 \right]. \quad (17)$$

Assumption 1 notably holds when \mathcal{F} is finite dimensional with $c^2 = \|K^{-1}\|_2^{-1} (\|K\|_2 + \lambda)$. As such all our lower-bound results can be cast with finite-dimensional approximation of infinite-dimensional RKHS. Under Assumption 1, we get

$$\begin{aligned} &\mathbb{E} \left[\left| \mathcal{B}_n - \theta_*^\top \Sigma_\lambda^{-2} \Sigma \theta_* \right| \mid \|F_n\| \leq 1/2 \right] \\ &\leq \sum_{i+j \neq 0} \left\| \Sigma_\lambda^{-1/2} (\Sigma_\lambda^{-1} \Sigma)^{1/2} \theta_* \right\|^2 \mathbb{E} \left[\left\| (\Sigma_\lambda^{-1} \Sigma)^{-1/2} F_n^i \Sigma_\lambda^{-1} \Sigma F_n^j (\Sigma_\lambda^{-1} \Sigma)^{-1/2} \right\| \mid \|F_n\| \leq 1/2 \right] \\ &\leq c^2 \sum_{i,j \in \mathbb{N}; i+j \neq 0} \left\| \Sigma_\lambda^{-1/2} (\Sigma_\lambda^{-1} \Sigma)^{1/2} \theta_* \right\|^2 \mathbb{E} \left[\|F_n\|^{i+j} \mid \|F_n\| \leq 1/2 \right], \end{aligned}$$

which allows us to proceed with the precedent derivations without assuming that (16) holds.

While the previous results were achieved for $f^* \in \mathcal{F}$, they can be extended by density to any f^* in the closure of \mathcal{F} in $L^2(\rho_{\mathcal{X}})$, i.e. $f^* \in (\ker K)^\perp$, leading to the following result.

Proposition 5. *When $f^* \in (\ker K)^\perp$ and $\lambda \leq \|\Sigma\|$, under the technical Assumption 1, the bias term can be bounded from above and below by*

$$|\mathbb{E}_{\mathcal{D}_n}[\mathcal{B}_n] - \mathcal{S}(\lambda)| \leq c^2 \mathcal{N}_1(\lambda) \left(\frac{56 \|f^*\|_2^2}{\lambda^2} \exp\left(-\frac{n}{6\mathcal{N}_\infty(\lambda)}\right) + \frac{8\mathcal{S}(\lambda)\mathcal{N}_\infty^{1/2}(\lambda)}{n^{1/2}} \right). \quad (18)$$

A.3.2 Discussion on the bias bound

More direct upper bound. The precedent derivations can be made more direct with the following series of implications, with $A \preceq B$ meaning that $x^\top Ax \leq x^\top Bx$ for every x :

$$\begin{aligned}
\|F_n\| \leq 1/2 &\Rightarrow -1/2I \preceq F_n \preceq 1/2I \\
&\Rightarrow 1/2I \preceq I - F_n \preceq 3/2I \\
&\Rightarrow 4/9I \preceq (I - F_n)^{-2} \preceq 4I \\
&\Rightarrow 4/9\mathcal{B}(\lambda) \preceq \theta_*^\top \Sigma^{1/2} \Sigma_\lambda^{-1} (I - F_n)^{-2} \Sigma_\lambda^{-1} \Sigma^{1/2} \theta_* \preceq 4\mathcal{B}(\lambda).
\end{aligned}$$

Let us assume that

$$\begin{aligned}
&\mathbb{E} \left[(I - F_n)^{-1} \Sigma \Sigma_\lambda^{-1} (I - F_n)^{-1} \mid \|F_n\| \leq 1/2 \right] \\
&\preceq c^2 \mathbb{E} \left[\Sigma^{1/2} \Sigma_\lambda^{-1/2} (I - F_n)^{-2} \Sigma^{1/2} \Sigma_\lambda^{-1/2} \mid \|F_n\| \leq 1/2 \right], \tag{19}
\end{aligned}$$

which is always verified for $c^2 = \min(\lambda^{-1}, \|K^{-1}\|_2^{-1}) \|K\|_2$ (although taking $c^2 \propto \lambda$ would slow down our upper bound by a factor of λ). This leads to the simple upper bound

$$\begin{aligned}
\mathcal{B}_n &= \theta_*^\top \Sigma_\lambda^{-1/2} (I - F_n)^{-1} \Sigma_\lambda^{-1} \Sigma (I - F_n)^{-1} \Sigma_\lambda^{-1/2} \theta_* \\
&\leq c^2 \theta_*^\top \Sigma_\lambda^{-1/2} (\Sigma_\lambda^{-1})^{1/2} (I - F_n)^{-2} (\Sigma_\lambda^{-1})^{1/2} \Sigma_\lambda^{-1/2} \theta_* + \|f^*\|_{L^2}^2 \mathbb{P}(\|F_n\| > 1/2) \\
&\leq 4c^2 \mathcal{S}(\lambda) + \|f^*\|_2^2 \mathcal{N}_1(\lambda) \exp\left(-\frac{n}{6\mathcal{N}_\infty(\lambda)}\right).
\end{aligned}$$

Improvement directions. In essence, we expect the bias upper-lower bound to behave as

$$\mathcal{S}(\lambda)(I - F_n)^{-2} - I \simeq \mathcal{S}(\lambda)F_n.$$

Getting this linear dependency in F_n explicitly would allow to improve the bound since

$$\mathbb{E}_{\mathcal{D}_n} [\|F_n\| \mid \|F_n\| \leq 1/2] \lesssim \mathcal{N}(\lambda) \mathcal{N}_\infty(\lambda) n^{-1}.$$

Moreover, going back to the definition of F_n ,

$$\begin{aligned}
\mathbb{E}_{\mathcal{D}_n} \theta_*^\top \Sigma \Sigma_\lambda^{-1} F_n \Sigma \Sigma_\lambda^{-1} \theta_* &= \mathbb{E}_{\mathcal{D}_n} \left[\left(\frac{1}{n} \sum_{i=1}^n \theta_*^\top \Sigma \Sigma_\lambda^{-3/2} \varphi(X_i) \right)^2 \right] - \mathbb{E}_X \left[\theta_*^\top \Sigma \Sigma_\lambda^{-3/2} \varphi(X) \right]^2 \\
&= \mathbb{E}_{\mathcal{D}_n} \left[\left(\frac{1}{n} \sum_{i=1}^n \theta_*^\top \Sigma \Sigma_\lambda^{-3/2} \varphi(X_i) - \mathbb{E}_X \left[\theta_*^\top \Sigma \Sigma_\lambda^{-3/2} \varphi(X) \right] \right)^2 \right],
\end{aligned}$$

which suggests possible improvements of the bound in $\mathcal{S}(\lambda)n^{-1}$.

A.3.3 Bounding the variance term

Let us now work on the term $\mathcal{V}_n = \text{Tr} \Sigma (\Sigma_n + \lambda)^{-2} \Sigma_n$. It works similarly to the bias term, concentrating towards $\mathcal{N}_2(\lambda)$. With $\Sigma_{n,\lambda} = \Sigma_n + \lambda I$, we have

$$\text{Tr} \left(\Sigma \Sigma_n \Sigma_{n,\lambda}^{-2} - \Sigma^2 \Sigma_\lambda^{-2} \right) = \text{Tr} \left(\Sigma \Sigma_\lambda^{-1} \Sigma_n \Sigma_{n,\lambda}^{-1} (\Sigma_{n,\lambda}^{-1} \Sigma_\lambda - I) + \Sigma \Sigma_\lambda^{-1} (\Sigma_n \Sigma_{n,\lambda}^{-1} - \Sigma \Sigma_\lambda^{-1}) \right).$$

Using that, for any A positive semi-definite and any B , $\text{Tr}(AB) \leq \|B\| \text{Tr}(A)$, it follows that

$$\begin{aligned}
|\mathcal{V}_n - \mathcal{N}_2(\lambda)| &\leq \mathcal{N}_1(\lambda) \left\| \Sigma_n \Sigma_{n,\lambda}^{-1} \right\| \left\| \Sigma_{n,\lambda}^{-1} \Sigma_\lambda - I \right\| + \mathcal{N}_1(\lambda) \left\| \Sigma_n \Sigma_{n,\lambda}^{-1} - \Sigma \Sigma_\lambda^{-1} \right\| \\
&\leq \mathcal{N}_1(\lambda) \left\| \Sigma_{n,\lambda}^{-1} \Sigma_\lambda - I \right\| + \mathcal{N}_1(\lambda) \left\| \Sigma_n \Sigma_{n,\lambda}^{-1} - \Sigma \Sigma_\lambda^{-1} \right\|.
\end{aligned}$$

Let us focus on the first term. Using $a^{-1} - b^{-1} = a^{-1}(b - a)b^{-1}$, we get

$$\begin{aligned}
\left\| \Sigma_\lambda \Sigma_{n,\lambda}^{-1} - I \right\| &= \left\| \Sigma_\lambda \Sigma_{n,\lambda}^{-1} (\Sigma - \Sigma_n) \Sigma_\lambda^{-1} \right\| \\
&\leq \left\| \Sigma_\lambda \Sigma_{n,\lambda}^{-1} \right\| \left\| \Sigma_\lambda^{1/2} F_n \Sigma_\lambda^{-1/2} \right\| \\
&\leq \left(\|I\| + \left\| \Sigma_\lambda \Sigma_{n,\lambda}^{-1} - I \right\| \right) \left\| \Sigma_\lambda^{1/2} F_n \Sigma_\lambda^{-1/2} \right\| \\
&\leq \sum_{i>0} \left\| \Sigma_\lambda^{1/2} F_n \Sigma_\lambda^{-1/2} \right\|^i.
\end{aligned}$$

For the second term,

$$\begin{aligned}
\left\| \Sigma_n \Sigma_{n,\lambda}^{-1} - \Sigma \Sigma_\lambda^{-1} \right\| &\leq \left\| \Sigma_n (\Sigma_{n,\lambda}^{-1} - \Sigma_\lambda^{-1}) \right\| + \left\| (\Sigma_n - \Sigma) \Sigma_\lambda^{-1} \right\| \\
&\leq \left\| \Sigma_n \Sigma_{n,\lambda}^{-1} (\Sigma - \Sigma_n) \Sigma_\lambda^{-1} \right\| + \left\| (\Sigma_n - \Sigma) \Sigma_\lambda^{-1} \right\| \\
&\leq 2 \left\| (\Sigma_n - \Sigma) \Sigma_\lambda^{-1} \right\| \\
&= 2 \left\| \Sigma_\lambda^{1/2} F_n \Sigma_\lambda^{-1/2} \right\|.
\end{aligned}$$

Similarly as for (16), if we assume that

$$\left\| \Sigma_\lambda^{1/2} F_n \Sigma_\lambda^{-1/2} \right\| \leq c \|F_n\|, \quad (20)$$

then we have, as long as $\|F_n\| \leq 1/2c$,

$$\begin{aligned}
|\mathcal{V}_n - \mathcal{N}_2(\lambda)| &\leq \sum_{i>0} \left\| \Sigma_\lambda^{1/2} F_n \Sigma_\lambda^{-1/2} \right\|^i + 2 \left\| \Sigma_\lambda^{1/2} F_n \Sigma_\lambda^{-1/2} \right\| \\
&\leq \frac{c \|F_n\|}{1 - c \|F_n\|} + 2c \|F_n\| \leq 4c \|F_n\|.
\end{aligned}$$

For the case when $\|F_n\|$ is large, we can again proceed with a simple bound:

$$|\mathcal{V}_n - \mathcal{N}_2(\lambda)| \leq \left| \text{Tr} \left(\Sigma \Sigma_n (\Sigma_n + \lambda)^{-2} \right) \right| + \text{Tr} \left(\Sigma^2 \Sigma_\lambda^{-2} \right) \leq 2 \text{Tr}(\Sigma) \lambda^{-1}.$$

Splitting the full expectation as we did for the bias we thus obtain

$$\begin{aligned}
|\mathbb{E}_{\mathcal{D}_n}[\mathcal{V}_n] - \mathcal{N}_2(\lambda)| &\leq \mathbb{E}_{\mathcal{D}_n}[|\mathcal{V}_n - \mathcal{N}_2(\lambda)|] \\
&\leq 2 \text{Tr}(\Sigma) \lambda^{-1} \mathbb{P}(\|F_n\| > 1/2c) + 4c \mathbb{E}[\|F_n\| \mid \|F_n\| \leq 1/2c] \mathbb{P}(\|F_n\| \leq 1/2c).
\end{aligned}$$

We are left with the computation of two integrals. As long as $\lambda \leq \|\Sigma\|$, with a the coefficient appearing in the exponential

$$\begin{aligned}
\mathbb{P}(\|F_n\| \leq 1/2c) \mathbb{E}[\|F_n\| \mid \|F_n\| \leq 1/2c] &\leq 28 \mathcal{N}_1(\lambda) \int_0^{1/2c} x \exp(-3nx^2/2\mathcal{N}_\infty(\lambda)) \, dx \\
&= 28 \mathcal{N}_1(\lambda) a^{-1} \int_0^{a^{1/2c}/2} x \exp(-x^2) \, dx \leq \frac{10 \mathcal{N}_1(\lambda) \mathcal{N}_\infty(\lambda)}{n}.
\end{aligned}$$

Once again, the condition (20) can be relaxed with the following assumption.

Assumption 2. *There exists a constant c such that, for all $i \in \mathbb{N}$,*

$$\mathbb{E} \left[\left\| \Sigma_\lambda^{1/2} F_n \Sigma_\lambda^{-1/2} \right\|^i \mid \|F_n\| \leq 1/2c \right] \leq c^i \mathbb{E} \left[\|F_n\|^i \mid \|F_n\| \leq 1/2c \right]. \quad (21)$$

As for Assumption 1, Assumption 2 holds when \mathcal{F} is finite-dimensional with $c^2 = \|K^{-1}\| (\|K\| + \lambda)$. It holds in general with $c^2 = \lambda^{-1}(\|\Sigma\| + \lambda)$, although this would deteriorate the bound by a factor of λ .

We are finally ready to collect the different pieces.

Proposition 6. *When $f^* \in (\ker K)^\perp$ and $\lambda \leq \|\Sigma\|$, under the technical Assumption 2, the variance term can be bounded from above and below by*

$$\frac{\varepsilon^2}{n} |\mathbb{E}_{\mathcal{D}_n}[\mathcal{V}_n] - \mathcal{N}_2(\lambda)| \leq \varepsilon^2 \mathcal{N}_1^2(\lambda) \left(\frac{28 \operatorname{Tr}(\Sigma)}{n\lambda} \exp\left(-\frac{c^2 n}{(4+2c)\mathcal{N}_\infty(\lambda)}\right) + \frac{40c\mathcal{N}_\infty(\lambda)}{n^2} \right). \quad (22)$$

A.3.4 Discussion to the variance bound

Once again, the bound presented here is somewhat unsatisfying, as it will not necessarily decrease faster than $\mathcal{N}(\lambda)/n$ if one considers target functions that are far away from \mathcal{F} and requires a large search space (i.e. $\mathcal{B}(\lambda)$ decreases slowly with λ , and given a fixed number of samples n the optimal λ_n is found for $\mathcal{N}(\lambda_n)$ quite large compared to n), so that $\mathcal{N}_\infty(\lambda)\mathcal{N}(\lambda)/n$ does not go to zero. Several directions can be taken to improve the bound. For example, when Y is bounded by M , the noise ε^2 can be replaced by M^2 , and it is possible to get an upper bound of the form

$$\mathbb{E}_{\mathcal{D}_n}[\mathcal{E}(f_{\lambda,n}^{(\text{thres.})})] \leq \frac{8M^2}{n} \mathcal{N}_1(\lambda) + \inf_{f \in \mathcal{F}} \left(\|f - f^*\|_{L^2}^2 + \lambda \|f\|_{\mathcal{F}}^2 \right),$$

for a truncated version $f_{\lambda,n}^{(\text{thres.})}$ of the estimator (6) as proved by Mourtada et al. [17] for ridge-less regression and extended to ridge regression in Mourtada et al. [18]. Moreover, retaking the analysis of Mourtada and Rosasco [16], one can get a lower bound of the form

$$\begin{aligned} \mathbb{E}_{\mathcal{D}_n} \mathcal{V}_n &\geq \frac{n}{n+1} \mathbb{E}_{\mathcal{D}_{n+1}} \operatorname{Tr} \left(\Sigma_n \Sigma_{n,\lambda}^{-1} \Sigma_{n+1} \Sigma_{n+1,\lambda(n+1)/n}^{-1} \right) \\ &\geq \frac{n}{n+1} \mathbb{E}_{\mathcal{D}_n} \operatorname{Tr} \left(\Sigma_n \Sigma_{n,\lambda}^{-1} \right) - \lambda \mathbb{E}_{\mathcal{D}_{n+1}} \operatorname{Tr} \left(\Sigma_n \Sigma_{n,\lambda}^{-1} \Sigma_{n+1,\lambda(n+1)/n}^{-1} \right), \end{aligned}$$

which might lead to some lower bound with

$$\begin{aligned} \mathbb{E}_{\mathcal{D}_{n+1}} \operatorname{Tr} \left(\Sigma_n \Sigma_{n,\lambda}^{-1} \Sigma_{n+1,\lambda(n+1)/n}^{-1} \right) &= \frac{n+1}{n} \mathbb{E}_{\mathcal{D}_n, X} \operatorname{Tr} \left(\Sigma_n \Sigma_{n,\lambda}^{-1} (\Sigma_{n,\lambda} + \varphi(X) \otimes \varphi(X))^{-1} \right) \\ &\leq \frac{n+1}{n} \mathbb{E}_{\mathcal{D}_n} \operatorname{Tr} \left(\Sigma_n \Sigma_{n,\lambda}^{-1} \right) \mathbb{E}_X \left[\|(\Sigma_{n,\lambda} + \varphi(X) \otimes \varphi(X))^{-1}\| \right]. \end{aligned}$$

We also note that it should not be too hard to replace F_n by $\Sigma^{1/2} \Sigma_\lambda^{-1} E_n \Sigma^{1/2} \Sigma_\lambda^{-1}$, which would lead to $\varepsilon^2 \mathcal{N}_2(\lambda)/n$ instead of $\varepsilon^2 \mathcal{N}_1(\lambda)/n$ in the right-hand side of (10).

A.4 Full theorem

Collecting the precedent results leads to the following theorem.

Theorem 3. *Under the technical Assumptions 1 and 2, as long as $\lambda \leq \|\Sigma\|$, when f^* belongs to the closure of \mathcal{F} in $L^2(\rho_X)$, the estimator (6) verifies*

$$\begin{aligned} \left| \mathbb{E}_{\mathcal{D}_n} [\mathcal{E}(f_{\lambda,n})] - \frac{\varepsilon^2 \mathcal{N}_2(\lambda)}{n} - \lambda^2 \mathcal{S}(\lambda) \right| &\leq \mathcal{N}_1(\lambda) \left(a_n \cdot \frac{\varepsilon^2 \mathcal{N}_1(\lambda)}{n} + a_n^{1/2} \lambda^2 \mathcal{S}(\lambda) \right) \\ &\quad + \mathcal{N}_1(\lambda) \left(\frac{\operatorname{Tr}(\Sigma) \varepsilon^2}{n} + \|f^*\|_{L^2}^2 \right) \exp(-ca_n), \end{aligned} \quad (23)$$

where $a_n = \mathcal{N}_\infty(\lambda)/n$.

As long as its right-hand side decreases faster than $\mathbb{E}_{\mathcal{D}_n}[\mathcal{E}(f_n)]$, Theorem 3 states that $\mathbb{E}_{\mathcal{D}_n}[\mathcal{E}(f_n)]$ behaves like

$$\mathbb{E}_{\mathcal{D}_n}[\mathcal{E}(f_n)] \simeq \frac{\varepsilon^2 \mathcal{N}_2(\lambda)}{n} + \lambda^2 \mathcal{S}(\lambda).$$

When optimizing for λ , assuming that $\mathcal{N}_1 \simeq \mathcal{N}_2$, the right-hand side of Theorem 3 decreases faster than $\mathbb{E}_{\mathcal{D}_n}[\mathcal{E}(f_n)]$ if and only if $\mathcal{N}_1(\lambda) a_n^{-1/2}$ goes to zero with n . This implies $\mathcal{N}(\lambda)^3 \leq n$, which is a much stronger condition than the high-sample regime condition $\mathcal{N}(\lambda) \leq n$.

A.4.1 Upper bound application to local polynomials

The following recalls a proof of convergence rates for local polynomial estimation. Consider the case where $\mathcal{X} = [0, 1]$ with uniform distribution, and $f = f^*$ is assumed to be (α, L) -Hölder,

$$|f^{(\lfloor \alpha \rfloor)}(x) - f^{(\lfloor \alpha \rfloor)}(y)| \leq L |x - y|^{\alpha - \lfloor \alpha \rfloor}.$$

Then, by fitting Taylor expansions on intervals $[(i-1)/m, i/m]$ for $i \in [m]$ and $m \in \mathbb{Z}_+$ with polynomials

$$\varphi(x) = \left(\left(x - \frac{2i-1}{2m} \right)^j \cdot \mathbf{1}_{x \in [\frac{i-1}{m}, \frac{i}{m}]} \right)_{i \in [m], j \in [0, \lfloor \alpha \rfloor]},$$

one can ensure that [see 11, Lemma 11.1]

$$\|\Pi_{\mathcal{F}} f^* - f^*\|_2 \leq \|\Pi_{\mathcal{F}} f^* - f^*\|_{\infty} \leq \frac{L}{2^{\alpha} \lfloor \alpha \rfloor! m^{\alpha}},$$

where $\Pi_{\mathcal{F}}$ denotes the orthogonal projection from L^2 onto \mathcal{F} . The same type of result also holds in dimension d using m^d multivariate polynomials of degree less than $\lfloor \alpha \rfloor$. The number of such polynomials is $m^d h_{\lfloor \alpha \rfloor}(1_d)$, where $h_{\lfloor \alpha \rfloor}$ is the complete homogeneous symmetric polynomial of degree $\lfloor \alpha \rfloor$ in d variables and 1_d is the vector of all ones. Thus,

$$h_{\lfloor \alpha \rfloor}(1_d) = \binom{d + \lfloor \alpha \rfloor}{\alpha} = \frac{(d + \lfloor \alpha \rfloor)!}{d! \lfloor \alpha \rfloor!} \geq \frac{\lfloor \alpha \rfloor^d}{d!}.$$

Balancing the bias and the variance term, we get an excess risk that behaves as

$$\mathbb{E} [\|f_n - f^*\|^2] \lesssim \inf_{m \in \mathbb{Z}_+} \frac{\varepsilon^2 m^d \lfloor \alpha \rfloor^d}{n} + \frac{L^2}{2^{2\alpha} \lfloor \alpha \rfloor! m^{2\alpha}} = c n^{-2\alpha/(d+2\alpha)},$$

for some constant c that depends on α , d and grows with L , σ^2 , the infimum being found for $m \propto (L^2 n)^{1/(d+2\alpha)}$. This shows an important point for practitioners: the size of the window should depend on how smooth f^* is expected to be among the functions in C^{α} .

Covering issues in high-dimension? Intuitively in high-dimension problems, where $d = \dim(\mathcal{X})$ is big, leveraging local properties is not very reasonable, since the covering of \mathcal{X} with local neighborhoods grows exponentially with the dimension d , meaning that if one wants to have enough samples per neighborhood, n should scale exponentially with d . Because rates in $O(n^{-2\alpha/(2\alpha+d)})$ are minimax optimal and of the lower bound in (10), it appears explicitly that to ensure minimax optimal convergence rates (i.e. make sure the rates hold for all functions in C^{α}), the partition size of \mathcal{X} should scale in $O(n^{d/(2\alpha+d)}) = O(n \times n^{-2\alpha/(2\alpha+d)})$ when trying to leverage the fact that $f^* \in C^{\alpha}$. Indeed and in contrast with the prior intuition, the partition size does not deteriorate with the dimension of the input space nor with the regularity of the target function, nor the percentage of the total volume contained in each region of the partition.² As a consequence, we expect the length of transitory regimes to suffer from the difficulty to leverage smoothness in high-dimension rather than to the fact that Taylor expansions need to be localized, and expect similar pessimistic pictures to take place when estimating target function through Fourier expansion.

²However, the radius of those regions will scale as $r = v^{1/d}$ for v the volume of those regions, meaning that when this volume will shrink to zero, the radius will shrink slower as the dimension grows, which will lead to a slower minimization of the approximation error.

A.4.2 Upper bound application to translation-invariant kernels

Table 1 depicts two types of kernels: the Matérn kernels (the exponential kernel corresponding to a Matérn kernel of low smoothness), and the Gaussian kernel (which can be seen as the limit of a Matérn kernel to infinite smoothness). By balancing bias and variance, one can prove the usual convergence rates for functions in Sobolev spaces, i.e. $f^* \in H^\alpha$. We refer to Appendix B for an explanation of those bounds on the variance and bias terms.

For the Matérn kernels, the generalization error reads, with $\tau = 2\beta - d$,

$$\mathbb{E} [\|f_n - f^*\|^2] \lesssim \frac{(\sigma^\tau \lambda)^{-d/2\beta}}{n} + (\sigma^\tau \lambda)^{\alpha/\beta}.$$

This is optimized for

$$\sigma^\tau \lambda = n^{-2\beta/(2\alpha+d)},$$

leading to minimax convergence rates in $O(n^{-2\alpha/(2\alpha+d)})$.

For the Gaussian kernel, we get

$$\mathbb{E} [\|f_n - f^*\|^2] \lesssim \frac{\sigma^{-d} \log(\lambda^{-1} \sigma^d)^{d/2}}{n} + \sigma^{2\alpha} \log(\lambda^{-1} \sigma^d)^{-\alpha},$$

which is optimized for

$$\sigma^{-2} \log(\lambda^{-1} \sigma^d) = n^{2/(2\alpha+d)},$$

leading to the same minimax convergence rate. In particular, when σ is fixed, this leads to

$$\lambda = \lambda_n = \sigma^d \exp(-\sigma^2 n^{2/(2\alpha+d)}).$$

Based on Theorem 2, this is true as long as $\mathcal{N}(\lambda) \mathcal{N}_\infty^{1/2}(\lambda)/n^{1/2}$ goes to zero with n , which imposes some constraints on α when assuming $f^* \in H^\alpha$. However, considering the refinement of Mourtada et al. [18], the upper bound is actually true without this constraint, which allows to prove the convergence rates in $O(n^{2\alpha/(2\alpha+d)})$ for any α .

A.4.3 Lower bound application to local polynomials - Proof of Proposition 1

Proposition 1 is a straightforward adaptation of Theorem 2, using the fact that $\mathcal{N}(0) = \dim \mathcal{F}$ is larger than the number of unknowns in a single Taylor expansion of order α in dimension d , which corresponds to the number of coefficients in a polynomial of degree α with d variables, and is equal to the number of sets of d elements among $d + \alpha$ elements.

A.4.4 Lower bound application to translation-invariant kernels - Proof of Proposition 2

Using the bias and variance lower bounds decomposition and Proposition 14, we get, when $f^* = f_m$ is a single frequency function $\hat{f}(\omega) = \delta_m(\omega)$ with $m \in \mathbb{Z}^d$,

$$\begin{aligned} \frac{\varepsilon^2 \mathcal{N}_2(\lambda)}{n} + \mathcal{B}(\lambda) &\geq \left(\frac{d\pi^{(d-1)/2}}{2^{d+2}\Gamma((d-1)/2)n} \lambda^{-d/2\beta} + \frac{\lambda^2}{((1 + \|m\|^2)^{-\beta} + \lambda)^2} \right) \\ &\geq \frac{1}{2} \left(\frac{d\pi^{(d-1)/2}}{2^{d+1}\Gamma((d-1)/2)n} \lambda^{-d/2\beta} + \min(\lambda^2(1 + \|m\|^2)^{2\beta}, 1) \right). \end{aligned}$$

From the fact that

$$\inf_{x \in \mathbb{R}} ax^{-\alpha} + bx^2 = \left(\alpha^{2/(2+\alpha)} + \alpha^{-\alpha/(2+\alpha)} \right) b^{\alpha/(2+\alpha)} a^{2/(2+\alpha)} \geq b^{\alpha/(2+\alpha)} a^{2/(2+\alpha)},$$

we have that, whatsoever λ is (if it is fixed for all n independently of the realization \mathcal{D}_n).

$$\begin{aligned} &\frac{d\pi^{(d-1)/2}}{2^{d+1}\Gamma((d-1)/2)n} \lambda^{-d/2\beta} + \lambda^2(1 + \|m\|^2)^{2\beta} \\ &\geq \left(\frac{d\pi^{(d-1)/2}}{2^{d-1}\Gamma((d-1)/2)} \right)^{4\beta/(4\beta+d)} \left(1 + \|m\|^2 \right)^{2\beta d/(4\beta+d)}. \end{aligned}$$

Once again, this lower bound is also true when d is replaced by any $l \in [d]$.

A.5 Interpolation spaces, capacity and source conditions

In this section, we discuss the values of $\mathcal{N}(\lambda)$ and $\mathcal{B}(\lambda)$ for classical problems.

A.5.1 Relation between variances

We begin with simple facts.

Proposition 7. *For any search space \mathcal{F} and regularization $\lambda > 0$,*

$$\mathcal{N}_2(\lambda) \leq \mathcal{N}_1(\lambda) \leq \mathcal{N}_\infty(\lambda). \quad (24)$$

Once again, the precise study of the variance is easier in \mathcal{H} with the operator Σ rather than in L^2 . First of all, notice that $K = SS^*$ has the same spectrum as $\Sigma = S^*S$, so that, for $a \in [1, 2]$,

$$\mathcal{N}_a(\lambda) = \text{Tr}((K + \lambda)^{-a} K^a) = \text{Tr}((\Sigma + \lambda)^{-a} \Sigma^a) = \sum_{\mu \in \text{spec}(\Sigma)} \frac{\mu^a}{(\lambda + \mu)^a}.$$

This shows the first part of the inequality (24):

$$\left(0 \leq \frac{x}{x + \lambda} \leq 1 \quad \Rightarrow \quad \frac{x}{x + \lambda} \leq \frac{x^a}{(x + \lambda)^a} \right) \quad \Rightarrow \quad \mathcal{N}_2(\lambda) \leq \mathcal{N}_1(\lambda).$$

For the second part of the inequality, we need to reformulate $\mathcal{N}_\infty(\lambda)$.

Lemma 8. *$\mathcal{N}_\infty(\lambda)$ can be expressed in \mathcal{H} as*

$$\mathcal{N}_\infty(\lambda) = \text{ess sup}_{x \sim \rho_{\mathcal{X}}} \left\| (\Sigma + \lambda)^{-1/2} \varphi(x) \right\|^2.$$

Proof. Observe that, for $x \in \mathcal{X}$,

$$\left\| (\Sigma + \lambda)^{-1/2} \varphi(x) \right\|^2 = \varphi(x)^\top (\Sigma + \lambda)^{-1} \varphi(x) = \text{Tr} \left((\Sigma + \lambda)^{-1} \varphi(x) \otimes \varphi(x) \right).$$

Let us introduce the operator

$$S_x : \mathcal{H} \rightarrow L^2(\rho_{\mathcal{X}}), \quad \theta \mapsto (x' \mapsto \varphi(x)^\top \theta).$$

From

$$\langle S_x \theta, g \rangle = \mathbb{E}[g(X) \varphi(x)^\top \theta] = \langle \theta, \mathbb{E}_X[g(X) \varphi(x)] \rangle$$

we get $S_x^* g = \mathbb{E}[g(X) \varphi(x)]$. Similarly, one can check that

$$K_x(g)(x') = (S_x S_x^* g)(x') = (S_x(\mathbb{E}_X[g(X) \varphi(x)]))(x') = \varphi(x)^\top \varphi(x) \mathbb{E}_X[g(X)] = \mathbb{E}[g] k(x, x),$$

and that

$$\Sigma_x \theta = S_x^* S_x \theta = \mathbb{E}_X[\varphi(x)^\top \theta] \varphi(x) = (\varphi(x) \otimes \varphi(x)) \theta,$$

from which we deduce that there exists $\varepsilon \in \{-1, 1\}$ such that

$$\varepsilon \left\| (K + \lambda)^{-1} K_x \right\| = \text{Tr}((K + \lambda)^{-1} K_x) = \text{Tr}((\Sigma + \lambda)^{-1} \varphi(x) \otimes \varphi(x)) = \left\| (\Sigma + \lambda)^{-1/2} \varphi(x) \right\|^2.$$

Necessarily $\varepsilon = 1$ since the right term is positive. Taking the essential supremum ends the proof. \square

In view of Lemma 8, the last inequality in (24) follows from

$$\mathcal{N}_2(\lambda) = \mathbb{E}_X [\text{Tr}((\Sigma + \lambda)^{-1} \varphi(X) \otimes \varphi(X))] \leq \text{ess sup}_X \text{Tr}((\Sigma + \lambda)^{-1} \varphi(X) \otimes \varphi(X)) = \mathcal{N}_\infty(\lambda).$$

A.5.2 Bounding the variance with interpolation inequalities

The following is a reinterpretation of Proposition 29 of Cabannes et al. [5].

Proposition 9 (Capacity condition). *When $K^p(L^2(\rho_{\mathcal{X}}))$ is continuously embedded in $L^\infty(\rho_{\mathcal{X}})$ with $p \leq 1/2$, there exists a constant c such that*

$$\mathcal{N}_\infty(\lambda) \leq c\lambda^{-2p}. \quad (25)$$

Proof. The continuous embedding means that there exists a constant c such that, for any $\lambda \geq 0$,

$$\|K^p f\|_\infty \leq c \|f\|_2.$$

Stated in \mathcal{H} , we get

$$\|S\theta\|_\infty \leq c \|K^{-p}S\theta\|_2 = c \|\Sigma^{1/2-p}\theta\|$$

for every $\theta \in \mathcal{H}$. In other terms,

$$\operatorname{ess\,sup}_x |\varphi(x)^\top \theta| \leq c \|\Sigma^{1/2-p}\theta\|.$$

Let us denote by (λ_i, θ_i) the eigenvalue decomposition of Σ . Then

$$\operatorname{ess\,sup}_x (\varphi(x)^\top \theta)^2 \leq c^2 \|\Sigma^{1/2-p}\theta\|^2 = c^2 \sum_{i \in \mathbb{N}} \lambda_i^{1-2p} (\theta_i^\top \theta)^2.$$

When considering $\theta = \theta_i$, this leads to

$$|\theta_i^\top \varphi(x)| \leq c\lambda_i^{1/2-p}.$$

Therefore,

$$\begin{aligned} \mathcal{N}_\infty^{1/2}(\lambda) &= \sup_x \left\| (\Sigma + \lambda)^{-1/2} \varphi(x) \right\| = \sup_x \sup_{\theta: \|\theta\| \leq 1} \theta^\top \Sigma_\lambda^{-1/2} \varphi(x) \\ &= \sup_x \sup_{\theta: \|\theta\| \leq 1} \sum_{i \in \mathbb{N}} \frac{\theta^\top \theta_i \theta_i^\top \varphi(x)}{(\lambda + \lambda_i)^{1/2}} \leq c \sup_{a: \sum a_i^2 \leq 1} \sum_{i \in \mathbb{N}} \frac{a_i \lambda_i^{1/2-p}}{(\lambda + \lambda_i)^{1/2}} \\ &= c \sup_{i \in \mathbb{N}} \frac{\lambda_i^{1/2-p}}{(\lambda + \lambda_i)^{1/2}} = c \sup_{t \in \operatorname{spec}(K)} \frac{t^{1/2-p}}{(\lambda + t)^{1/2}} \leq c \sup_{t \geq 0} \frac{t^{1/2-p}}{(\lambda + t)^{1/2}} \\ &= c(2p)^{-p} (1 - 2p)^{1/2-p} \lambda^{-p}, \end{aligned}$$

where the last equality follows from basic calculus. \square

A.5.3 Bounding the bias with source conditions

We now focus our attention on the bias term.

Proposition 10 (Capacity condition). *When $f^* \in K^q(L^2(\rho_{\mathcal{X}}))$ with $q \leq 1$, there exists a constant c such that, for any $\lambda \geq 0$,*

$$\mathcal{B}(\lambda) = \lambda^2 \mathcal{S}(\lambda) \leq c\lambda^{2q}. \quad (26)$$

Proof. The proof is straight-forward. If $f^* = K^q g$ with $g \in L^2$, then

$$\begin{aligned} \mathcal{S}(\lambda) &= \|(K + \lambda)^{-1} f^*\|_2 = \|(K + \lambda)^{-1} K^q g\|_2 \\ &= \|(K + \lambda)^{q-1}\|_2 \|(K + \lambda)^{-q} K^q g\|_2 \leq \lambda^{q-1} \|K^{-p} f^*\|_2. \end{aligned}$$

Squaring this term and multiplying it by λ^2 leads to the result. \square

A.5.4 Classical interpolation inequalities

We begin with a simple proposition.

Proposition 11. *When the function $x \rightarrow k(x, x)$ is bounded, the RKHS associated with k verifies*

$$\mathcal{N}_\infty(\lambda) = O(\lambda^{-1}).$$

Proof. This follows from the fact that $K^{1/2}(L^2) \hookrightarrow L^\infty$ as soon as φ is bounded since, for any $f = \varphi(\cdot)^\top \theta \in \mathcal{F} = S\mathcal{H} = K^{1/2}(L^2)$,

$$|f(x)| = |\varphi(x)^\top \theta| \leq \|\varphi\|_\infty \|\theta\| = \|\varphi\|_\infty \|f\|_{\mathcal{F}} = \|\varphi\|_\infty \left\| K^{-1/2} f \right\|_2.$$

The previous characterization of \mathcal{N}_∞ leads to the claim. \square

We now turn ourselves to more complicated interpolations, and offer an informal proposition of facts that are well-known in approximation theory [28, 9].

Proposition 12 (Informal source condition). *When $\mathcal{F} = H^\beta$ and $f^* \in H^\alpha$, it holds*

$$f^* \in K^{\alpha/2\beta}(L^2(\rho_{\mathcal{X}})).$$

Proof. In essence, as explained in Appendix B, K takes a function in $L^2(\rho_{\mathcal{X}})$ and multiply its Fourier transform by $\hat{q}(\omega)^{-1} = (1 + \|\omega\|^2)^\beta$, with q defining the Matérn kernel, making it 2β -smooth in the Sobolev sense. In harmonic settings where the Fourier functions diagonalize K and $\hat{q}(\omega)$ parameterizes the spectrum of K , the fractional operator K^p can be seen as multiplying the Fourier transform of f by $\hat{q}(\omega)^{-p}$, making it $2p\beta$ -smooth. This fact can be extended beyond those harmonic settings, notably with interpolation inequalities as the one used for the last part of Proposition 3. On the opposite direction, any α -smooth function can be multiplied by $q(\omega)^{\alpha/2\beta}$ in Fourier while staying in $L^2(\rho_{\mathcal{X}})$, so that, if f^* is α -smooth, it belongs to $K^{\alpha/2\beta}$. \square

Proposition 13 (Informal interpolation inequality). *When $\mathcal{F} = H^\beta$ is the space of α -Sobolev functions,*

$$K^{d/2\beta}(L^2) \hookrightarrow L^\infty.$$

Proof. Note that $\mathcal{F} = S\mathcal{H} = K^{1/2}(L^2)$. We have seen informally in the proof of the previous lemma how $K^p(L^2 \subset H^{2p\beta})$. Now, let us recall the Sobolev embedding theorems [1]. Under mild assumptions on $\rho_{\mathcal{X}}$, for $k, r, l, s > 0$

$$W^{k,r}(\rho_{\mathcal{X}}) \hookrightarrow W^{l,s}(\rho_{\mathcal{X}}), \quad \text{as long as} \quad \frac{1}{r} - \frac{k}{d} \leq \frac{1}{s} - \frac{l}{d}.$$

We want to use it with $k = 2p\beta$, $r = 2$, $l = 0$ and $s = +\infty$, which leads to $p = 4\beta/d$. \square

These results partially explained Table 1, which we derive formally in Appendix B.

B Translation-invariant kernels and Fourier analysis

Let us recall basic facts about kernel methods and Fourier analysis, before providing proofs to Propositions 2 and 3.

B.1 Stylized analysis on the torus

When k is a translation-invariant kernel, i.e. $k(x, x') = q(x - x')$, the integral operator K is a convolution against q . Let us expand on the friendly case provided by the torus $\mathcal{X} = \mathbb{T}^d := \mathbb{R}^d / \mathbb{Z}^d = [0, 1]^d / \sim$, where \sim is the relation identifying opposite faces of the hypercube, and $\rho_{\mathcal{X}}$ the uniform distribution. On the torus, a translation invariant kernel is defined through q being a one-periodic function on \mathbb{R}^d . Let dx denote the Lebesgue measure on \mathbb{R}^d . The integral operator $K : L^2(\mathcal{X}, dx) \rightarrow L^2(\mathcal{X}, dx)$ is the convolution

$$Kf(x) = \int_{[0,1]^d} k(x, x') f(x') dx' = \int_{[0,1]^d} q(x' - x) f(x') dx' = q * f(x).$$

For $m \in \mathbb{Z}^d$, define the Fourier function $f_m : x \mapsto \exp(2i\pi \langle m, x \rangle)$. One can check that the f_m 's form an orthonormal family that diagonalizes K with³

$$Kf_m = \hat{q}_m f_m, \quad \text{where} \quad \hat{q}_m = \int_{[0,1]^d} q(x) \exp(2i\pi \langle x, m \rangle) dx.$$

Hence, using Pythagoras theorem, we can define the norm on \mathcal{F} through its action on Fourier coefficients as

$$\|f\|_{\mathcal{F}}^2 = \langle f, K^{-1}f \rangle_{L^2(\rho_{\mathcal{X}})} = \sum_{m \in \mathbb{Z}^d} \hat{q}_m^{-1} |\hat{f}_m|^2 = \int_{\mathbb{R}^d} \hat{q}(\omega)^{-1} |\hat{f}(\omega)|^2 \#(d\omega),$$

where $\hat{f}_m = \langle f, f_m \rangle_{L^2(\rho_{\mathcal{X}})}$, and $\#$ is the counting measure on $\mathbb{Z}^d \subset \mathbb{R}^d$.

B.1.1 First part of the proof of Proposition 3

Since K is diagonalized in Fourier, we compute the size of \mathcal{F} for $a \in \{1, 2\}$ with

$$\mathcal{N}_a(\lambda) = \text{Tr} (K^a (K + \lambda)^{-a}) = \sum_{m \in \mathbb{Z}^d} \frac{\hat{q}_m^a}{(\hat{q}_m + \lambda)^a}.$$

For kernels whose scales are explicitly defined through $q_{\sigma} = q(x/\sigma)$, we have $\hat{q}_{\sigma}(\omega) = \sigma^d \hat{q}(\sigma\omega)$, which leads to (12).

Similarly, the bound on the bias term follows from Fourier analysis by

$$\mathcal{B}(\lambda) = \|K(K + \lambda)^{-1}f - f\|_{L^2(\rho_{\mathcal{X}})}^2 = \sum_{m \in \mathbb{Z}^d} \left| \hat{f}_m \right| \left(\frac{\hat{q}_m}{\hat{q}_m + \lambda} - 1 \right)^2 = \sum_{m \in \mathbb{Z}^d} \left| \hat{f}_m \right| \left(\frac{\lambda}{\hat{q}_m + \lambda} \right)^2,$$

which provides (13).

B.1.2 Second part of the proof of Proposition 3

When ρ is a distribution that is absolutely continuous with respect to the Lebesgue measure and whose density is bounded from above, we get

$$K \preceq \rho_{\infty} K_{dx}, \quad \text{with} \quad \rho_{\infty} = \left\| \frac{d\rho_{\mathcal{X}}}{dx} \right\|_{L^{\infty}(\rho_{\mathcal{X}})},$$

where K_{dx} is the integral operator associated to the kernel k on $L^2(dx)$. Using the fact the effective dimension is an increasing function of the eigenvalues (since $x \mapsto x/(x+1)$ is increasing), and that eigenvalues are increasing with the Loewner order, this leads to

$$\mathcal{N}(\lambda) \leq \rho_{\infty} \text{Tr} ((K_{dx} + \lambda)^{-1} K_{dx}) = \rho_{\infty} \int_{\mathbb{R}^d} \frac{\hat{q}(\omega)}{\lambda + \hat{q}(\omega)} d\omega.$$

³Indeed, the Fourier transform of a function $f \in L^2(\mathbb{T}^d)$ can be defined as the mapping from \mathbb{N} to $(\langle f_i, f \rangle)_{i \in \mathbb{N}}$ where (f_i) is a basis that diagonalizes all convolution operators (note that this definition is possible because $\rho_{\mathcal{X}}$ is uniform on the torus).

Note that those derivations are written informally (since K and K_{dx} do not act on the same space), but could be made formal with the isomorphic covariance operators on \mathcal{H} , plus some technicalities to make sure Σ_{dx} is well defined (assuming $\varphi(X)$ has a fourth-order moment against Lebesgue, or approaching K_{dx} within its action on compact subspaces of \mathcal{X} where it is bounded, before taking the limit of $\mathcal{N}_{dx}(\lambda)$).

For the bias term, using the fact that $L^2(\rho_{\mathcal{X}})$ is continuously embedded in $L^2(dx)$ and the isometry between the spatial and the Fourier domain, we get

$$\|f - f^*\|_{L^2(\rho_{\mathcal{X}})} \leq \rho_{\infty}^{1/2} \|f - f^*\|_{L^2(dx)} = \rho_{\infty}^{1/2} \|\widehat{f} - \widehat{f}^*\|_{L^2(dx)}.$$

Finally, it should be noted that the norm associated with \mathcal{F} does not depend on the density of X , hence the formula can be written independently of $\rho_{\mathcal{X}}$. Indeed, under definition assumption, i.e. if $q \in L^1(dx)$, this formula can even be written with a measure of infinite mass. For example, when $\mathcal{X} = \mathbb{R}^d$, one can consider the Fourier transform associated with $L^2(dx)$, and get

$$\|f\|_{\mathcal{F}}^2 = \int_{\mathbb{R}^d} \widehat{q}(\omega)^{-1} |\widehat{f}(\omega)|^2 d\omega, \quad \text{where} \quad \widehat{q}(\omega) = \int_{\mathbb{R}^d} q(x) \exp(-2i\pi \langle x, \omega \rangle) dx, \quad (27)$$

although some care is needed to deal with the continuous version of the spectral theorem (the set of eigenvalues being non-countable). From there the same derivations as for Proposition 3 lead to the desired result.

B.2 Sobolev spaces

Recall the action of differentiation on the Fourier transform: for $m \in \mathbb{N}^d$, $|m| := \|m\|_1$, and $f \in L^2(dx)$,

$$\frac{\widehat{\partial^{|m|} f}}{\prod_{i \in [d]} \partial^{m_i} x_i}(\omega) = (2i\pi)^{|m|} \prod_{i \in [d]} \omega_i^{m_i} \widehat{f}(\omega).$$

This characterizes the pseudo-norm

$$\|f\|_m^2 = \int_{\mathbb{R}^d} \left\| \frac{\partial^{|m|} f(x)}{\prod_{i \in [d]} \partial^{m_i} x_i} \right\|^2 dx = (2\pi)^{2|m|} \int_{\mathbb{R}^d} \prod_{i \in [d]} \omega_i^{2m_i} |\widehat{f}(\omega)|^2 d\omega.$$

This pseudo-norm is associated with the translation-invariant kernel such that $\widehat{q}(\omega) = \prod_{i \in [d]} \omega_i^{-2m_i}$ as per (27). Note that q is well defined when \widehat{q} belongs to $L^1(dx)$ (by Bochner's theorem), that is $|m| > d$. Those observations are usual to deduce that the Matérn kernels, which are defined from $\widehat{q}(\omega) \propto (1 + \|\omega\|_2^2)^{-\beta}$, correspond to the Sobolev spaces $H^{\beta}(dx)$ endowed with the norm

$$\|f\|_{H^{\beta}}^2 = \sum_{m; |m| \leq \beta} \|f\|_m^2.$$

It follows from Bochner's theorem that H^{β} is a reproducing kernel Hilbert space if and only if $2\beta > d$. Remarkably, the exponential kernel corresponds to the Matérn kernel with $\beta = (d+1)/2$ [22]. For the Gaussian kernel, $\widehat{q}(\omega) = \pi^{-d/2} \exp(-\pi^2 \|\omega\|^2)$, and the associated function class \mathcal{F} is analytic (by the Paley-Wiener theorem).

B.2.1 Functional sizes

Let us now express the capacity and bias bound within Sobolev spaces.

Proposition 14 (Sobolev capacity). *When $\widehat{q}(\omega) = (1 + \|\omega\|^2)^{-\beta}$ for $\beta > d$, $\lambda\sigma^{-d}$ is bounded and ρ has a bounded density, we have*

$$\mathcal{N}_1(\lambda, \sigma) \leq \frac{2\beta \rho_{\infty} \pi^{(d+1)/2}}{\Gamma((d-1)/2)} \lambda^{-d/2\beta} \sigma^{-d(2\beta-d)/2\beta}.$$

Moreover, when $\mathcal{X} = \mathbb{T}^d$ and $\rho_{\mathcal{X}}$ is uniform, we get

$$\mathcal{N}_2(\lambda, \sigma = 1) \geq \max_{l \in [d]} \frac{l \pi^{(l+1)/2}}{2^{l+1} \Gamma((l-1)/2)} \lambda^{-l/2\beta}.$$

Proof. In this setting, Proposition 3 leads to

$$\begin{aligned} \int_{\mathbb{R}^d} \frac{1}{1 + \lambda \widehat{q}_{\sigma}(\omega)^{-1}} d\omega &= \int_{\mathbb{R}^d} \frac{1}{1 + \lambda \sigma^{-d} \widehat{q}(\sigma \omega)^{-1}} d\omega = \int_{\mathbb{R}^d} \frac{1}{1 + \lambda \sigma^{-d} (1 + \sigma^2 \|\omega\|^2)^{\beta}} d\omega \\ &= \text{surf}(\mathcal{S}^{d+1}) \int_{\mathbb{R}_+} \frac{r^{d-1} dr}{1 + \lambda \sigma^{-d} (1 + \sigma^2 r^2)^{\beta}} \\ &= 2\pi \text{vol}(\mathcal{S}^d) \int_{\lambda^{1/\beta} \sigma^{-d/\beta}}^{\infty} \frac{(u - \lambda^{1/\beta} \sigma^{-d/\beta})^{d/2-1} du}{\lambda^{d/2\beta} \sigma^{d-d^2/2\beta} (1 + u^{\beta})} \\ &= 2\pi \text{vol}(\mathcal{S}^d) \lambda^{-d/2\beta} \sigma^{d(d-2\beta)/2\beta} \int_{\mathbb{R}_+} \frac{x^{d/2-1} dx}{1 + (x + \lambda^{1/\beta} \sigma^{-d/\beta})^{\beta}} \\ &\leq 2\pi \beta \text{vol}(\mathcal{S}^d) \lambda^{-d/2\beta} \sigma^{d(d-2\beta)/2\beta}, \end{aligned}$$

where we used the fact that

$$\begin{aligned} \int_0^{\infty} \frac{x^{d/2-1} dx}{1 + (x + \lambda^{1/\beta} \sigma^{-d/\beta})^{\beta}} &\leq \int_0^{\infty} \frac{x^{d/2-1} dx}{\max(1, \max(x^{\beta}, \lambda \sigma^{-d}))} \\ &\leq \int_0^1 x^{d/2-1} dx + \int_1^{\infty} \frac{x^{d/2-1} dx}{x^{\beta}} = d/2 - (d/2 - \beta) = \beta, \end{aligned}$$

which is true as long as $\beta > d/2$ to ensure proper convergence of the last integral.

For the part on the torus, in order to get a sharp learning limit, we need to be slightly more precise. In particular, we want to relate the discrete Fourier transform integral of Proposition 3 with the continuous one through series-integral comparison, and get a lower bound on the last integral. We will fix $\sigma = 1$ for simplicity. A simple cut of \mathbb{R}^d into unit cubes, together with the fact that our integrand is decreasing, leads to

$$\sum_{m \in \mathbb{Z}^d} \mathbf{1}_{0 \notin m} \frac{\widehat{q}_m^2}{(\widehat{q}_m + \lambda)^2} \leq \int \frac{\widehat{q}(\omega)^2}{(\widehat{q}(\omega) + \lambda)^2} d\omega \leq \sum_{m \in \mathbb{Z}^d} 2^{\#\{i \in [d] \mid m_i = 0\}} \frac{\widehat{q}_m^2}{(\widehat{q}_m + \lambda)^2}.$$

We simplify it as

$$\mathcal{N}_2(\sigma, \lambda) \geq 2^{-d} \int \frac{\widehat{q}(\omega)^2}{(\widehat{q}(\omega) + \lambda)^2} d\omega.$$

We now compute the integral with the same techniques as before:

$$\begin{aligned} \int \frac{\widehat{q}(\omega)^2}{(\widehat{q}(\omega) + \lambda)^2} d\omega &= \int \frac{1}{(1 + \widehat{q}(\omega)^{-1} \lambda)^2} d\omega = \int \frac{1}{(1 + (1 + \|\omega\|^2)^{\beta} \lambda)^2} d\omega \\ &= 2\pi \text{vol}(\mathcal{S}^d) \int \frac{x^{d-1}}{(1 + (1 + x^2)^{\beta} \lambda)^2} dx \\ &= 2\pi \text{vol}(\mathcal{S}^d) \lambda^{-d/2\beta} \int \frac{x^{d-1}}{(1 + (\lambda^{1/\beta} + x^2)^{\beta})^2} dx \\ &\geq 2\pi \text{vol}(\mathcal{S}^d) \lambda^{-d/2\beta} \int \frac{x^{d-1}}{4 \max(1, 4^{\beta} \max(\lambda^2, x^{4\beta}))} dx \\ &= 2^{-1} \pi \text{vol}(\mathcal{S}^d) \lambda^{-d/2\beta} \left(\int_0^1 x^{d-1} dx + 4^{-\beta} \int_1^{\infty} \frac{x^{d-1}}{x^{4\beta}} dx \right) \\ &= 2^{-1} \pi \text{vol}(\mathcal{S}^d) \lambda^{-d/2\beta} (d + 4^{-\beta} (4\beta - d)) \\ &\geq 2^{-1} \pi \text{vol}(\mathcal{S}^d) \lambda^{-d/2\beta} d. \end{aligned}$$

It should be noted that this last bound is somewhat too lax, as it tends to zero when the dimension increases. Since $\sum_{m \in \mathbb{Z}^d} a(\|m\|)$ for $a > 0$ is strictly increasing with d , we deduce that this lower bound holds for any $k \leq d$. \square

Proposition 15 (Gaussian capacity). *When $\widehat{q}(\omega) = \exp(-\|\omega\|^2)$ and ρ has a bounded density, we have*

$$\mathcal{N}_1(\lambda, \sigma) \leq \frac{\rho_\infty \pi^{(d-1)/2} d}{2\sigma^d} L(\lambda^{-1} \sigma^d),$$

where L is defined by Eq. (28). In particular, $L(x) \leq x$ when $x < 1$, and $L(x) \lesssim \log(x)^{d/2}$ when x gets large. Moreover when $\mathcal{X} = \mathbb{T}^d$ and $\rho_{\mathcal{X}}$ is uniform, we get

$$\mathcal{N}_2(\lambda, \sigma) \geq \frac{\pi^{(d-1)/2}}{2^{d+1} \sigma^d} L(\lambda^{-1} \sigma^d).$$

Proof. With the Gaussian kernel, Proposition 3 leads to

$$\begin{aligned} \int_{\mathbb{R}^d} \frac{1}{1 + \lambda \sigma^{-d} \exp(\sigma^2 \|\omega\|^2)} d\omega &= \text{vol}(\mathbb{S}^d) \int_{\mathbb{R}_+} \frac{2x^{d-1}}{1 + \lambda \sigma^{-d} \exp(\sigma^2 x^2)} dx \\ &= \text{vol}(\mathbb{S}^d) \sigma^{-d} \int_{\mathbb{R}_+} \frac{u^{d/2-1}}{1 + \lambda \sigma^{-d} \exp(u)} du \\ &= \text{vol}(\mathbb{S}^d) \Gamma(d/2) \frac{-\text{Li}_{d/2}(-\sigma^d/\lambda)}{\sigma^d}, \end{aligned}$$

where $\text{Li}_{d/2}$ is the polylogarithm function, hence the definition of L as

$$L(x) = -\text{Li}_{d/2}(-x) = \sum_{k=1}^{\infty} \frac{(-1)^{k+1} x^k}{k^{d/2}}. \quad (28)$$

We recognize an alternating sequence, whose term amplitudes are decreasing as a function of $k \in \mathbb{N}$ when $x \leq 1$, which explains that $L(x)$ is smaller than the first term in this case. The expansion of the polylogarithm function at infinity leads to the upper bound when x goes to infinity.

When it comes to a lower bound, we can proceed as the precedent lemma with

$$\mathcal{N}_2(\sigma, \lambda) \geq 2^{-d} \int \frac{d\omega}{(1 + \lambda \widehat{q}(\omega)^{-1})^2} \geq 2^{-d} \int \frac{d\omega}{1 + \lambda \widehat{q}(\omega)^{-1}},$$

which corresponds to the integral computed for the upper bound. Once again, this also holds when d is replaced by any $l \in [d]$. \square

B.2.2 Adherence

Let us now turn our attention to the bias, i.e. the adherence of functions in those spaces. For proof readability, we will assume that $\rho_{\mathcal{X}}$ has compact support. In this setting, $W^{\alpha,2}$ is continuously embedded in $C^{\alpha+d/2} = W^{\alpha+d/2,\infty}$, which can be defined as

$$C^{\alpha+d/2} = \left\{ f : \mathbb{R}^d \rightarrow \mathbb{R} \mid \|f\|_{\alpha} := \text{ess sup}_{\omega \in \mathbb{R}^d} |\widehat{f}(\omega)| (1 + \|\omega\|)^{\alpha+d/2} < +\infty \right\}.$$

Proposition 16 (Adherence of H^{α} in H^{β}). *When $\widehat{q}(\omega) = (1 + \|\omega\|^2)^{-\beta}$, hence $\mathcal{F} = H^{\beta}$, if $\alpha > 2\beta$, for any $f^* \in H^{\alpha}(\rho_{\mathcal{X}})$, and λ small enough, we have*

$$\mathcal{B}(\sigma, \lambda) \leq \lambda^2 \|K^{-1} f\|_{L^2(\rho_{\mathcal{X}})}^2.$$

If $\alpha < \beta$ and $\rho_{\mathcal{X}}$ has a bounded density, then for any function $f^* \in C^{\alpha+d/2}$

$$\mathcal{B}(\sigma, \lambda) \leq \rho_{\infty} \frac{4\beta \pi^{(d+1)/2} \rho_{\infty} \|f\|_{\alpha}^2 \beta}{(\beta^2 - \alpha^2) \Gamma((d-1)/2)} \lambda^{\alpha/\beta} \sigma^{(2\beta-d)\alpha/\beta}. \quad (29)$$

Proof. The first part results from previous considerations on the source condition since we have the inclusion $f^* \in H^\alpha \subset H^{2\beta} = K(L^2(\rho_\chi))$. The second part follows from an $L^1 - L^\infty$ Hölder inequality:

$$\begin{aligned}
\mathcal{B}(\sigma, \lambda) &\leq \rho_\infty \int_{\mathbb{R}^d} \frac{|\widehat{f}(\omega)|^2}{(\lambda^{-1}\sigma^d \widehat{q}(\sigma\omega) + 1)^2} d\omega \leq \rho_\infty \|f\|_\alpha^2 \int_{\mathbb{R}^d} \frac{(1 + \|\omega\|^2)^{-(d/2+\alpha)}}{(\lambda^{-1}\sigma^d(1 + \sigma^2 \|\omega\|^2)^{-\beta} + 1)^2} d\omega \\
&= 2\pi \text{vol}(\mathbb{S}^d) \rho_\infty \|f\|_\alpha^2 \int_{\mathbb{R}_+} \frac{2(1+x^2)^{-(d/2+\alpha)} x^{d-1}}{(\lambda^{-1}\sigma^d(1 + \sigma^2 x^2)^{-\beta} + 1)^2} dx \\
&= 2\pi \text{vol}(\mathbb{S}^d) \rho_\infty \|f\|_\alpha^2 a^\alpha \sigma^{2\alpha} \int_a^\infty \frac{(u-a+a\sigma^2)^{-(d/2+\alpha)} (u-a)^{d/2-1}}{(u^{-\beta} + 1)^2} du \\
&\leq \frac{4\beta\pi \text{vol}(\mathbb{S}^d) \rho_\infty \|f\|_\alpha^2 \beta}{\beta^2 - \alpha^2} \lambda^{\alpha/\beta} \sigma^{(2\beta-d)\alpha/\beta},
\end{aligned}$$

where a was set to $\lambda^{1/\beta} \sigma^{-d/\beta}$, and the last integral can be bounded by

$$\begin{aligned}
&\int_a^\infty \frac{(u-a+a\sigma^2)^{-(d/2+\alpha)} (u-a)^{d/2-1}}{(u^{-\beta} + 1)^2} du \leq \int_0^\infty \frac{u^{d/2+\beta-1}}{(u+a(\sigma^2-1))^{d/2+\alpha} (1+u^\beta)^2} du \\
&\leq \int_0^\infty \frac{u^{d/2+\beta-1}}{(u+a(\sigma^2-1))^{d/2+\alpha} (1+u^\beta)^2} du \leq \int_0^1 \frac{u^{d/2+\beta-1}}{u^{d/2+\alpha}} du + \int_1^{+\infty} \frac{u^{d/2+\beta-1}}{u^{d/2+\alpha} u^2 \beta} du \\
&= \frac{1}{\beta-\alpha} + \frac{1}{\beta+\alpha} = \frac{\beta}{\alpha(\beta-\alpha)}.
\end{aligned}$$

Recalling the volume of the sphere completes the proof. \square

Proposition 17 (Adherence of H^α in the Gaussian RKHS). *When \mathcal{F} is associated with the Gaussian kernel and ρ_χ has a bounded density, for any $f^* \in C^{\alpha+d/2}$ we have*

$$\mathcal{B}(\sigma, \lambda) \leq \frac{2\pi^{(d+1)/2} \rho_\infty \|f\|_\alpha^2}{\Gamma((d-1)/2)} \left(\frac{1}{\sigma^{2d+4\alpha}} + \frac{2 \log(2)^{-(d/2+2\alpha)}}{d+2\alpha} \right) \sigma^{2\alpha} \log(\lambda^{-1}\sigma^d)^{-\alpha}.$$

Proof. We follow the same path as for the adherence of H^α in H^β :

$$\begin{aligned}
\mathcal{B}(\sigma, \lambda) &\leq \rho_\infty \|f\|_\alpha^2 \int_{\mathbb{R}^d} \frac{(1 + \|\omega\|^2)^{-(d/2+\alpha)}}{(\lambda^{-1}\sigma^d \widehat{q}(\sigma\omega) + 1)^2} d\omega \\
&= \rho_\infty \|f\|_\alpha^2 \int_{\mathbb{R}^d} \frac{(1 + \|\omega\|^2)^{-(d/2+\alpha)}}{(\lambda^{-1}\sigma^d \exp(-\sigma^2 \|\omega\|^2) + 1)^2} d\omega \\
&= 2\pi \text{vol}(\mathbb{S}^d) \rho_\infty \|f\|_\alpha^2 \int_{\mathbb{R}_+} \frac{(1+x^2)^{-(d/2+\alpha)} x^{d-1}}{(\lambda^{-1}\sigma^d \exp(-\sigma^2 x^2) + 1)^2} dx \\
&= 2\pi \text{vol}(\mathbb{S}^d) \rho_\infty \|f\|_\alpha^2 \sigma^{2\alpha} \int_1^{+\infty} \frac{\log(x)^{d/2-1}}{(\sigma^2 + \log(x))^{d+2\alpha} (a+x)} dx \\
&\leq 2\pi \text{vol}(\mathbb{S}^d) \rho_\infty \|f\|_\alpha^2 \sigma^{2\alpha} \log(\lambda^{-1}\sigma^d)^{-\alpha} \left(\frac{1}{\sigma^{2d+4\alpha}} + \frac{\log(2)^{-\alpha}}{\alpha} \right),
\end{aligned}$$

where the integral can be bounded by

$$\begin{aligned}
\int_1^{+\infty} \frac{\log(x)^{d/2-1}}{(\sigma^2 + \log(x))^{d+2\alpha} (a+x)} dx &\leq \int_1^e \frac{\log(x)}{\sigma^{2d+4\alpha}} dx + \int_e^{+\infty} \frac{1}{(\log(x))^{d/2+2\alpha+1} x} dx \\
&= \frac{1}{\sigma^{2d+4\alpha}} + \frac{\log(2)^{-(d/2+2\alpha)}}{d/2+2\alpha}.
\end{aligned}$$

The same type of derivations can be made for the bias in the lower bound. \square

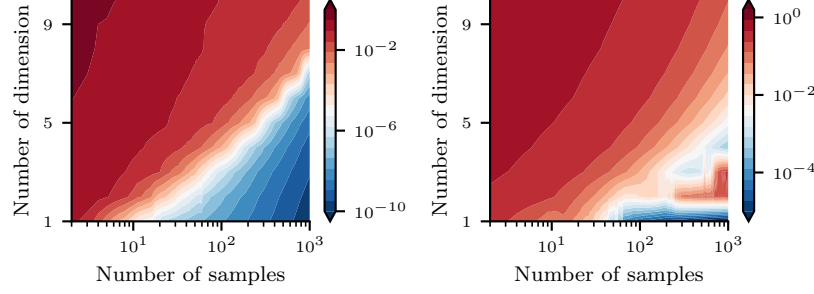


Figure 7: (Right) Noise-free convergence rates for $f^*(x) = x_1^5$ with $k(x, y) \propto (1 + x^\top y)^5$. We observed similar deterioration of convergence rates as a function of the dimension d as on Figure 2. The fact that the error is not exactly zero when $d = 1$ and $n \geq 5$ is due to a small regularization added in our algorithm to avoid running into computational issues when inverting a matrix online. (Left) Convergence rates for $f^*(x) = \cos(4\pi x_1)$ on the torus $\mathcal{X} = \mathbb{T}^d$ with the (periodic) exponential kernel $k(x, y) = q(-100 \|x - y\|^2 / d)$. We observe similar behavior as on Figure 2, the picture being worse because the kernel weights all frequencies in the Fourier domain, and not only the first $\binom{d+5}{5}$ ones.

Note that the proofs also work when the $L^1 - L^\infty$ Hölder inequality is replaced with $L^\infty - L^1$, showcasing the norm of f in H^α instead of in $C^{\alpha+d/2}$. We refer to Bach [4] for details.

Remark 18 (Blessing of dimensionality). *It should be noted that all our integral calculations show a constant $2\pi\rho_\infty \text{vol}(\mathbb{S}^d)$ which will be present in front of the excess risk. As d increases, this constant goes to zero faster than any exponential profile. To see that, note how the volume of the d -sphere is always smaller than twice the one of its inscribed hypercube, whose volume is $d^{-d/2}$. We do not have clear intuition to understand this behavior at the time of writing.*

C Experimental details

C.1 Online solving of problems of increasing size

In order to solve a big number of least-squares problems with increasing numbers of samples, one can use recursive matrix inversion. When $A \in \mathbb{R}^{n \times n}$, $x \in \mathbb{R}^n$ and $b \in \mathbb{R}$, one can check that

$$\begin{pmatrix} A & x \\ x^\top & b \end{pmatrix}^{-1} = \begin{pmatrix} A^{-1} + cyy^\top & -cy \\ -cy^\top & c \end{pmatrix},$$

where

$$c = \frac{1}{b - x^\top y}, \quad \text{and} \quad y = A^{-1}x.$$

This allows efficient computation of matrix inversion online as the number of samples increases.

C.2 Example of convergence rates for “sparse” functions

Polynomial estimation. Consider the target function $f^*(x) = 63x_1^5 - 70x_1^3 + 15x_1$, learned with the polynomial kernel $k(x, y) = (1 + x^\top y)^p$ with $p = 5$ on $\mathcal{X} = [0, 1]^d$ and $\rho_{\mathcal{X}}$ uniform, in the interpolation regime $\lambda = 0$. In this setting, \mathcal{F} is exactly the space of polynomials of degree no larger than 5, which follows from the fact that k can be rewritten through a vector φ that enumerates monomials:

$$(1 + x^\top y)^p = \sum_{i=0}^p \binom{p}{i} \sum_{(i_j)_j: \sum_j i_j = i} \binom{i}{(i_j)_j} \prod x_j^{i_j} y_j^{i_j} = \varphi(x)^\top \varphi(y).$$

As a consequence, f^* belongs to \mathcal{F} , and we expect the bias term to be zero. Yet, we expect the variance, hence the generalization error, to behave as $\varepsilon^2 \dim \mathcal{F} / n$, where ε corresponds to some

notion of variability between labels. The dimension of the class of polynomials in dimension d of degree no larger than p is $\binom{p+d}{d}$. In particular, in dimension $d = 100$, a polynomial of degree at most $p = 5$ can have up to one hundred million coefficients, so that one needs about one hundred million observations to enter the high-sample regime and expect an excess risk $\mathcal{E}(f_n)$ of order ε^2 as per Theorem 2. While one could fit a polynomial of lower maximum degree, e.g. 4 instead of 5, since the f^* considered here is actually orthogonal to all polynomials of lower degree, there is no hope to obtain better rates. On Figure 2, the target function is $f^*(x) = x_1^5$, and the polynomial kernel is normalized as

$$k(x, y) = \left(\frac{1 + x^\top y}{1 + d} \right)^5$$

to avoid computational issues. The noise level ε is set to 10^{-2} , and the lower bound in $\varepsilon^2 \dim \mathcal{F}/n$ is plotted on Figure 2. In practice, this lower bound describes well the learning dynamic when the number of samples is high compared to the effective dimension of the space of functions considered.

Same examples in Fourier. To transpose the previous example in the Fourier domain, one can consider $f^*(x) = \cos(\omega_0 x_1)$ together with some translation-invariant kernel. We illustrate this case on Figure 7. The deterioration of the rates with respect to dimension can be understood precisely. In harmonic settings, such as on the torus with uniform measure, one can consider f^* as an eigenfunction of the integral operator K associated with the eigenvalue λ_{ω_0} . The lower bound on the bias is given by

$$\mathcal{B} = \frac{\lambda^2}{(\lambda + \lambda_{\omega_0})^2}.$$

When k is translation-invariant, $k(x, y) = q(x - y)$, we get that

$$\text{Tr}(K) = \sum_{\omega \in \mathbb{Z}^d} \lambda_\omega = \text{Tr}(\mathbb{E}[\varphi(X)\varphi(X)^\top]) = \mathbb{E}[\varphi(X)^\top \varphi(X)] = \mathbb{E}[k(X, X)] = q(0).$$

When $q(0)$ does not depend on d , this quantity is constant. On the other hand, we expect λ_ω to decrease with $\|\omega\|$. But since the number of frequencies below $\|\omega_0\|$ grows exponentially with the dimension, in order to keep this sum constant λ_{ω_0} has to decrease exponentially fast with the dimension, hence the bias will increase exponentially fast with the dimension.

Example of “wrongfully” arbitrarily fast convergence rates. To further emphasize the importance of constants and transitory regimes, let us discuss an even simpler example. Assume that one wants to learn a polynomial of a unknown degree $s \in \mathbb{N}$ in a noiseless setting; or equivalently, learn an analytical function such that $f^{(s+1)} = 0$ for an unknown $s \in \mathbb{N}$. This polynomial can be learned exactly when provided with as many points as the unknown coefficients in the polynomial, meaning that the generalization error will almost surely goes to zero when provided enough points. As a consequence,

$$\forall h : \mathbb{N} \rightarrow \mathbb{R}, \quad \mathcal{E}(f_n) \leq O(h(n)),$$

where f_n is defined in (5) with \mathcal{F} the space of polynomials of any degree. In other terms, we are able to prove *arbitrarily fast convergence rates*. Yet, such convergence rates hide constants that are the real quantities governing convergence behaviors of any learning procedure. Figure 7 shows how the number of coefficients in a Taylor expansion of order s is once again the right quantity to look at.

C.3 Different convergence rates profiles

Figure 3 was computed with the Gaussian kernel on either the one-dimensional torus or \mathbb{R} . One hundred runs were launched and averaged to get a meaningful estimate of the expected excess risk. Convergence rates were computed for different hyperparameters, and the best set of hyperparameters (changing with respect to the number of samples but constant over run) was taken to show the best achievable convergence rate.

Fast then slow profile. Let us focus on the example provided by $f^* : x \mapsto \exp(-\max(x^2, M)) - \exp(-M)$ (note that we subtract $\exp(-M)$ so that the function goes to zero at infinity, which remove

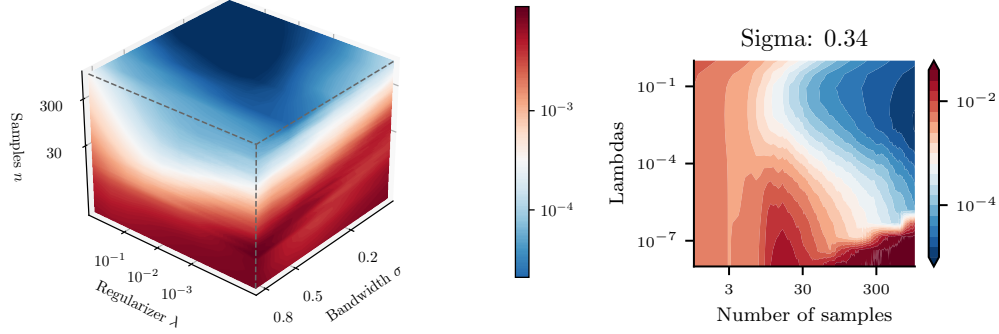


Figure 8: Excess risk when the target at the top is taken as $f^*(x) = \exp(-\max(x^2, M)) - \exp(M)$ with $M = 1/4$, and $x \in \mathbb{R}$ with unit Gaussian distribution. Note that the learning of the smooth part is more efficient when the regularizer is big, which forces the reconstruction to be smooth.

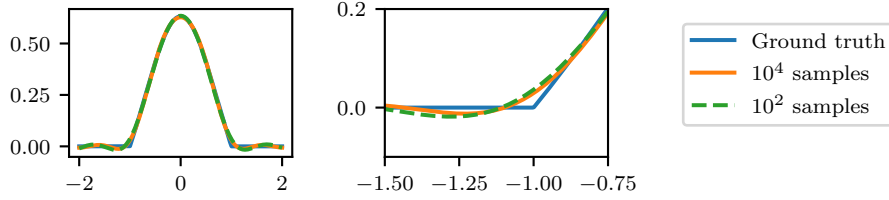


Figure 9: Example of a smooth target function with a C^1 -singularity whose estimation is expected to showcase convergence rates that decrease first fast and then slowly. The x -axis represents the input space $\mathcal{X} = [-2, 2]$, the y -axis represent the output space $f^*(x)$ and $f_{n,\lambda}$ for $n = 10^2$ and $n = 10^4$. The first fast decrease of excess risk corresponds to the easy estimation of the coarse details of the function, while the slow decrease thereafter corresponds to the precise estimation of the C^1 -singularity. The target function $x \mapsto \exp(-\max(x^2, 1)) - \exp(-1)$ is represented in blue, the estimation with 10^4 samples is represented in orange, and the one with 10^2 samples is represented in dashed green. The left picture zooms in on the estimation of the singularity. We see that the increase from 10^2 to 10^4 does not lead to a much better estimate.

the burden of learning a constant offset with the Gaussian kernel). Note that, for $q_\sigma = \exp(-x^2/\sigma)$, the convolution $q_\sigma * f$ for a large σ will not modify f much, while making it analytical. This follows from Fourier analysis: if f is integrable, its Fourier transform is bounded; since a convolution corresponds to a product in Fourier, and since the Fourier transform of q_σ decays exponentially fast, so does $f * q_\sigma$, which implies its analytical property. As a consequence, all functions are close to analytical functions, whose approximation should exhibit convergence rates in $O(n^{-1})$. In particular, for f^* defined as before for a some M large enough, without enough observations one will not be able to distinguish between f^* and $q_\sigma * f^*$, and as the number of sample first increases, one will learn quite fast a smooth version of f^* . After a certain number of samples, the learning will stall until enough points are provided to distinguish between f^* and its smoothing, and learn the C^1 -singularity of the former. Figures 8 and 9 illustrate this observation. Note that similar reasoning could be made for any RKHS that is dense in $L^2(\rho_{\mathcal{X}})$.

Slow then fast profile. The slow then fast profile was computed with $\mathcal{X} = \mathbb{S}^1$, $\rho_{\mathcal{X}}$ being uniform and $f^* : x \mapsto \cos(2\pi\omega x)$ with $\omega = 20$. One hundred runs were launched and averaged to get an estimate of the excess risk of the estimator in (6) for different values of σ and λ . Again, the best results for different sample sizes were reported to get an estimate of convergence rates on Figure 3. A log-log-log-log plot of the results is provided on Figure 10.

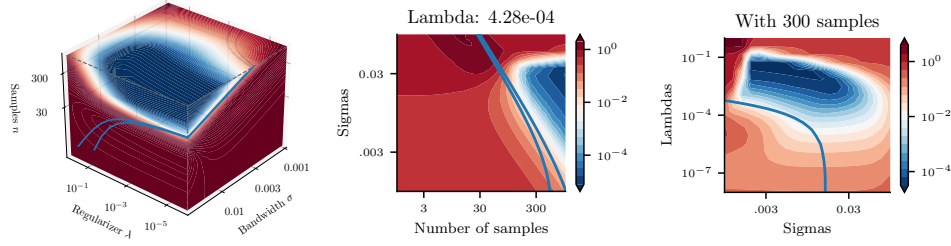


Figure 10: Excess of risk when the target at the top is taken as $f^*(x) = \cos(2\pi\omega x)$ with $\omega = 20$, and $x \in \mathbb{S}^1 = \mathbb{R}/\mathbb{Z}$ uniform on the circle. Observe how the risk first stalls, before learning the function quite fast. The two graphs $\{(n, \mathcal{N}_a(\lambda, \sigma))\}$ for $a \in \{1, 2\}$ are plotted with the blue lines.

C.4 Exploring the low-sample regime

Looking at the population weights first. When given access to the knowledge of the full distribution ρ , the estimator in (6) can be rewritten as

$$f_{\infty, \lambda} = \mathbb{E}[Y \alpha_X], \quad \alpha_X : x \rightarrow (K + \lambda I)^{-1} k(X, x). \quad (30)$$

This shows an interesting property of kernel ridge regression: it can be seen as learning in an unsupervised fashion the weights $\alpha : \mathcal{X} \rightarrow L^2(\rho)$, which then indicate how to fold the input space to use information provided by the labels. At a high level, one can think of a scheme, given some input points, to perform finite differences and leverage the result to build an estimate of the target function from Taylor expansions, whatsoever would be the label observations. Figure 11 shows how, when λ is not too big, the reconstruction $f_{\infty, \lambda}(x_0)$ (x_0 being the same point at the bluest center on the different pictures on this Figure) depends on observations made far away from x_0 according to some periodic pattern, implicitly assuming that the target function should be regular when looked at in the Fourier domain. From this picture, one can build examples of non-smooth functions where this inductive bias will have adversarial effects.

Looking at the empirical weights. While the previous paragraph discusses the weights $\alpha_X(x)$ when given access to the full distribution, similar derivations can be made when accessing a finite number of samples. Indeed, kernel ridge regression reads as

$$f_{\lambda, n}(x) = \sum_{i \in [n]} Y_i \hat{\alpha}_i(x), \quad \hat{\alpha}(x) = (\hat{K} + n\lambda)^{-1} \hat{K}_x \in \mathbb{R}^n,$$

where

$$\hat{K} = (k(X_i, X_j))_{i, j \in [n]} \in \mathbb{R}^{n \times n}, \quad \hat{K}_x = (k(X_i, x))_{i \in [n]} \in \mathbb{R}^n.$$

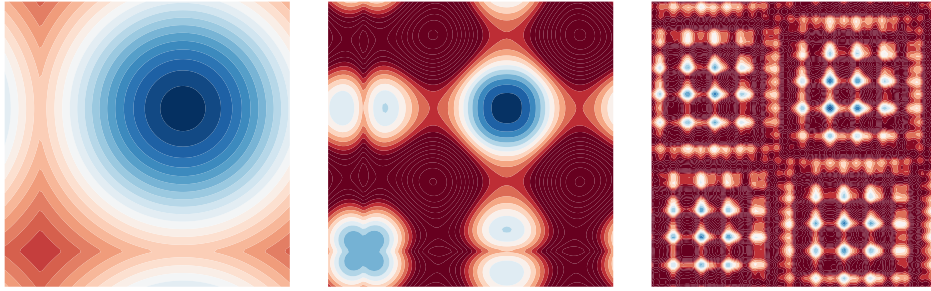


Figure 11: Level lines of the weights $x \rightarrow \alpha_x(x_0)$ (30) for a given $x_0 \in \mathcal{X}$, when \mathcal{X} is the torus $\mathbb{R}^2/[-1, 1]^2$ and the kernel is taken as the Gaussian kernel with the Riemannian metric on the torus (think of an unrolled donut). Parameters are taken as $\sigma = 1$ together with $\lambda = 10^6$ (left), $\lambda = 10^2$ (middle) or $\lambda = 1$ (right).

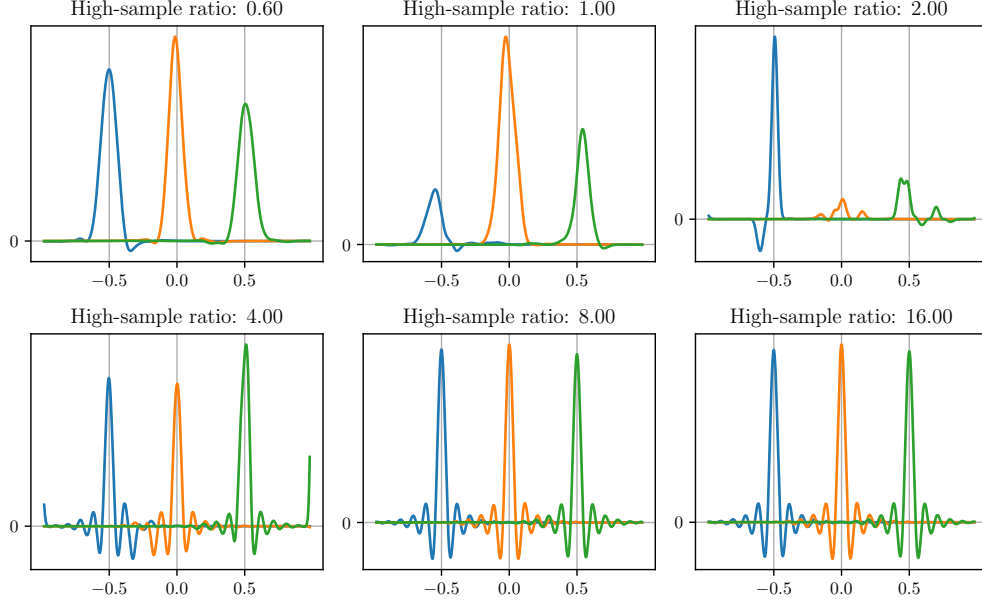


Figure 12: Weights $x \mapsto \hat{\alpha}_X(x)$ as per (30), for $X = -1/2$ (blue), $X = 0$ (orange) and $X = 1/2$ (green), when $\mathcal{X} = [-1, 1]$ and $\rho_{\mathcal{X}}$ is uniform. The weights are computed with the Gaussian kernel with bandwidth $\sigma = .1$ and $\lambda = 10^{-5}$, which yields an effective dimension $\mathcal{N} = 45$, and for $n \in \{27, 45, 90, 180, 360, 720\}$, which explains the high-sample ratio n/\mathcal{N} seen on the title of the different plots. When this ratio is close to one, the weights present weird behaviors, which could explain the picture observed in convergence rates when transitioning from low-sample to high-sample regimes.

Note that $\hat{\alpha}_i(x) = \hat{\alpha}_{X_i|\mathbb{X}}(x)$ where $\mathbb{X} = (X_1, \dots, X_n)$ is the input dataset. As a consequence,

$$\mathbb{E}_{\mathcal{D}_n}[f_n(x)] = \sum_{i \in [n]} \mathbb{E}_{\mathcal{D}_n}[Y_i \hat{\alpha}_{X_i|\mathbb{X}}(x)] = n \cdots \mathbb{E}_{\mathcal{D}_n}[Y_1 \hat{\alpha}_{X_1|\mathbb{X}}(x)].$$

In other terms, f_n is a bias estimator whose average is defined as

$$\mathbb{E}_{\mathcal{D}_n}[f_n] = \mathbb{E}_{(X,Y)}[Y \hat{\alpha}_X], \quad \hat{\alpha}_X = n \cdot \mathbb{E}_{\mathbb{X}}[\hat{\alpha}_{X_1|\mathbb{X}} | X_1 = X]. \quad (31)$$

These are the weights plotted on Figures 12 and 13. In order to compute those weights efficiently, one can use the block matrix inversion. Using the sliced indices matrix notations, we have

$$\begin{aligned} \hat{\alpha}_{X_n|\mathcal{D}_n}(x) &= [(\hat{K} + n\lambda)^{-1} \hat{K}_X]_n = [(\hat{K} + n\lambda)^{-1}]_{n,:} \times \hat{K}_x \\ &= [(\hat{K} + n\lambda)^{-1}]_{n,:n-1} \times [\hat{K}_x]_{:n-1} + [(\hat{K} + n\lambda)^{-1}]_{n,n} \times [\hat{K}_x]_n \\ &= -(b - x^\top A^{-1}x)^{-1} ([\hat{K}_x]_n - x^\top A^{-1} \times [\hat{K}_x]_{:n-1}). \end{aligned}$$

where

$$\hat{K} + n\lambda I = \begin{pmatrix} A & x \\ x^\top & b \end{pmatrix} = \begin{pmatrix} [\hat{K}]_{:n-1,:n-1} + n\lambda & [\hat{K}]_{n,:n-1} \\ [\hat{K}]_{n,:n-1}^\top & [\hat{K}]_{n,n} + n\lambda \end{pmatrix}.$$

Denoting

$$\tilde{K} = (k(X_i, X_j))_{i,j \in [n-1]} \in \mathbb{R}^{n-1 \times n-1} \quad \tilde{K}_x = (k(X_i, x))_{i \in [n-1]} \in \mathbb{R}^{n-1},$$

we get

$$\hat{\alpha}_{X|\mathcal{D}_n}(x) = (k(X, X) - Z_X^\top Z_X + n\lambda)^{-1} (k(X, x) - Z_X^\top Z_x), \quad Z_x = (\tilde{K} + n\lambda)^{-1/2} \tilde{K}_x.$$

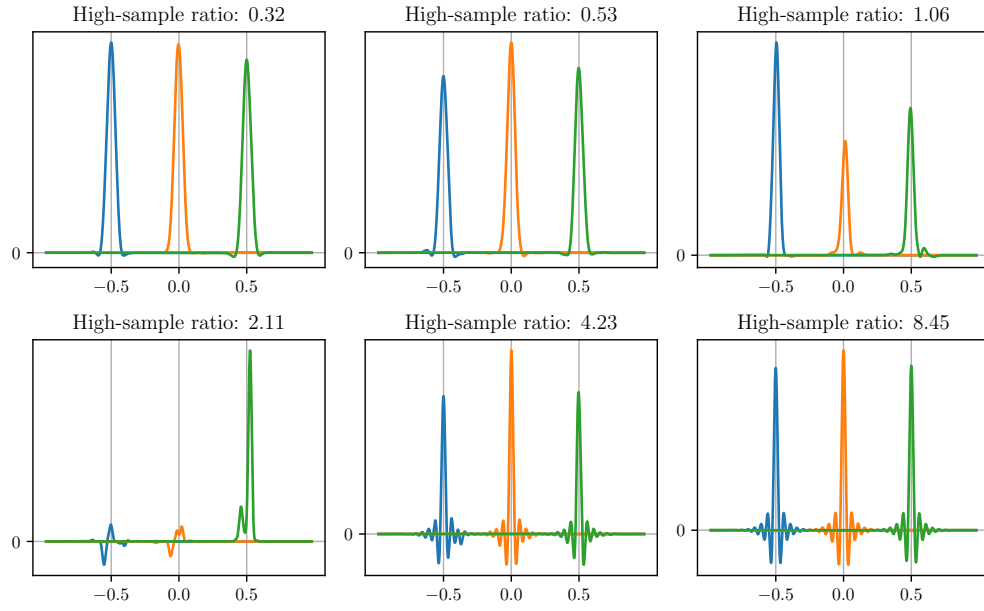


Figure 13: Same picture as Figure 12 yet with $\sigma = .05$, which leads to an effective dimension $\mathcal{N} = 85$.